Electronics Research Laboratory
University of California
Berkeley, California

THE MEASUREMENTS OF THE SCATTERED PATTERNS OF THE FERRITE POST

by

C. Y. Fong

Supported in part by the
Air Force Office of Scientific Research
of the Office of Aerospace Research;
Department of the Army, Army Research Office;
and Department of the Navy, Office of Naval Research
Grant No. AF-AFOSR-62-340

January 25, 1962

TABLE OF CONTENTS

		Page
I.	INTRODUCTION	1
II.	ARRANGEMENTS	1
III.	THEORETICAL CONSIDERATIONS	3
IV.	MEASUREMENT RESULTS AND THEIR RELATION TO THE THEORY	17
	REFERENCES	40

I. INTRODUCTION

Ferrites are compounds with the chemical formula MFe_2O_4, where M is a divalent metal such as magnesium, manganese, zinc, iron, or cobalt. They have high resistivities in the order of 10^6 ohm-cm. The most important property of ferrites is their permeability. The permeability is not a constant but is a function of the externally applied magnetic field (d-c magnetic field). This causes the ferrites to exhibit nonreciprocal properties. In these measurements, two ferrite samples (R-1 type, i.e., Mg-Mn ferrite) are used to scatter a plane wave of frequency of 9372 mc/sec. We measured the scattered field patterns for different applied static magnetic fields. The nonreciprocal property of the ferrite yields measured patterns which are not symmetric to the axis of the transmitting antenna. When we reverse the applied magnetic field, the patterns are mirror images of those with the original d-c field.

II. ARRANGEMENTS

The schematic diagram of the experimental apparatus is shown in Figure 1.

In Fig. 2, each of the ground plates is made of four 5' x 5' sheets of seamless aluminum bonded to a 1" thick aluminum honeycomb. The edges are filled with epoxy plastic. The spacing between the two ground plates is 0.5" which is maintained by cylindrical brass spacers so that only the TEM mode wave can propagate for the X-band operation. In order to make an electrically infinite parallel plate region, a 5' diameter annular wooden ring into which the wedge-shaped absorbers are inserted radially, is placed between the plates. A horn used as the transmitting antenna is inserted between the ground plates by cutting a small part of the annular wooden ring. A 28" diameter cast aluminum turntable is mounted flush with the lower plate. A spring-like arrangement of brass finger-stock attaches the rim of the turntable to the lower plate. The angular position of the turntable is determined by the degree scale along the underside of the turntable and a fixed marker. A standard electric probe used

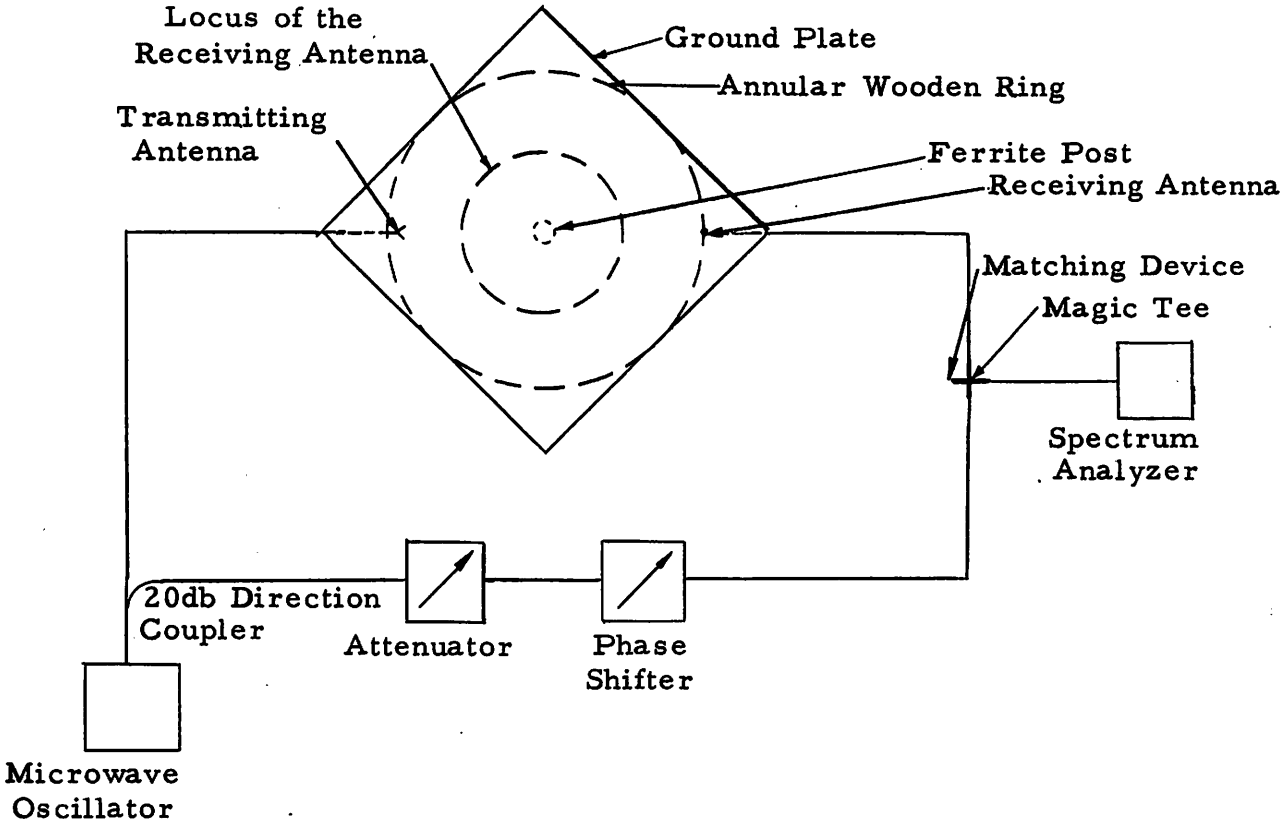

Fig. 1 Schematic diagram of the arrangement for the measurements.

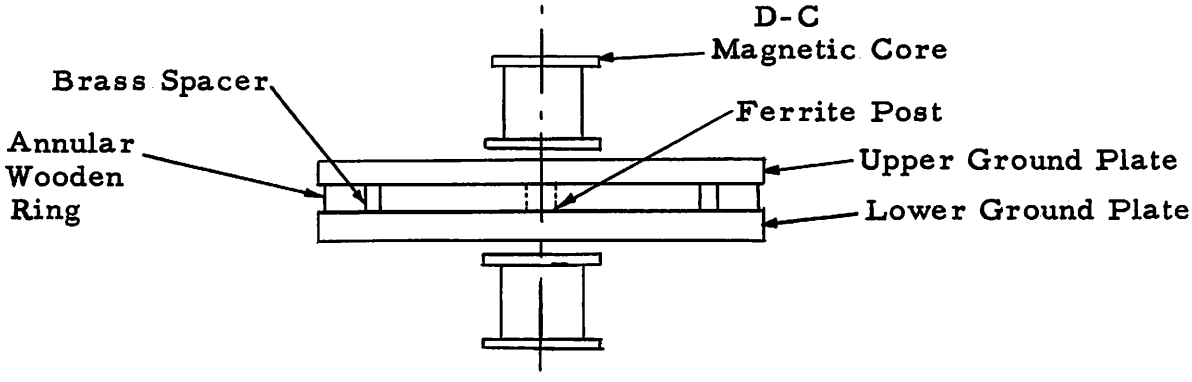

Fig. 2 Side view of the arrangement of the ground plate.

as a receiving antenna is mounted in a brass plug which fits snugly in the turntable. The position of the receiving antenna can be obtained from the degree scale of the turntable. The center part of the turntable with diameter 3" can be removed, so that we can take the ferrite out of the ground plates and put it back again without disturbing the upper ground plate. The static magnetic field along the axis of the ferrite post is provided by an electromagnet, one leg of which is on the upper plate and the other under the lower plate. The current in the winding of the electromagnet is supplied by a d-c power supply (not shown in Fig. 2).

The total field pattern (the incident field pattern plus the scattered field pattern) is obtained by using a bridge circuit to null the signal in the spectrum analyzer as shown in Fig. 1. The bridge circuit is made of two arms. One arm consists of X-band waveguides, the horn, the space between the ground plates, the receiving antenna, and one arm of the magic tee. The other arm includes a 20-db direction coupler, the X-band waveguides, the attenuator, the phase shifter, and one arm of the magic tee. One of the other two arms of the magic tee is connected to the matching device and the other to the spectrum analyzer (which serves as a sensitive detector).

To check the correct frequency, a modulator and a frequency meter are inserted in the system before the 20-db direction coupler. An 800 c/sec. audio signal is applied to the modulator. By setting the frequency meter to 9372 c/sec. and tuning the microwave oscillator circuit, we find the dip in the output of an audio voltmeter which, with a crystal detector, replaces the spectrum analyzer for this particular test.

III. THEORETICAL CONSIDERATIONS

Because the parallel ground plates form the image of the ferrite post, we can consider this to be the problem of a plane wave normally incident on an infinitely long cylindrical ferrite post magnetized uniformly along its axis, i. e., the Z-axis. The magnetic field vector $\vec{H}$ of the plane wave is perpendicular to the static magnetic field $\vec{H}_o$ as shown in Fig. 3.

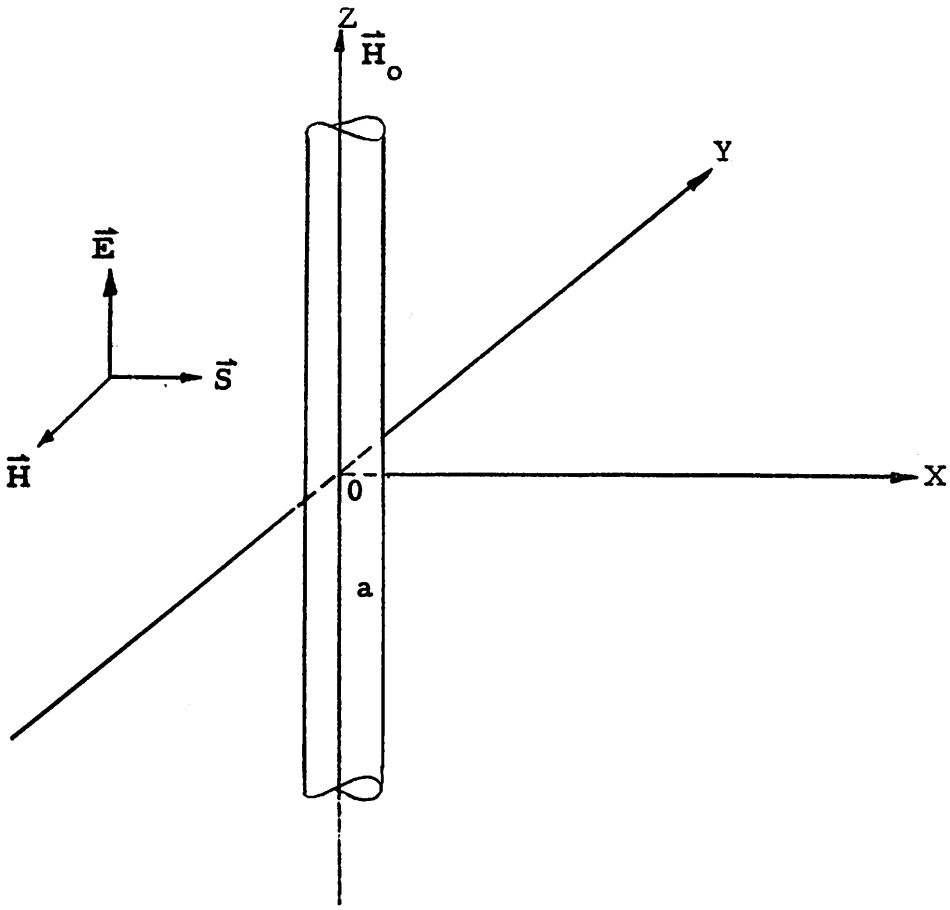

Fig. 3 Plane wave is incident on (normally) an infinitely long cylindrical ferrite post, magnetized uniformly along its axis.

When the ferrite is magnetized by the strong d-c magnetic field and the r-f alternating magnetic field $\vec{H}$ at frequency ω at right angles to the static field $\vec{H}_o$, the magnetization vector $\vec{M}$ precesses at frequency ω around $\vec{H}_o$, as shown in Fig. 4. This causes the magnetization $\vec{M}$ inside the ferrite to

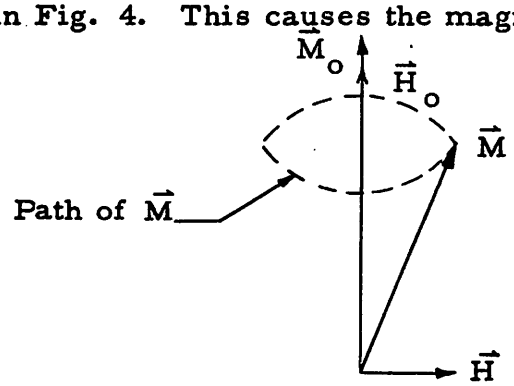

Fig. 4 Diagram of precession of magnetization M.

be not in the same direction with the r-f magnetic field $\vec{H}$. Polder[1] derived the tensor form of the permeability of the ferrite by considering the simple classical model of the precessing magnetic moment of the electron in a magnetic field. We use the following form:

$$[\mu] = \begin{bmatrix} \mu & jk & 0 \\ jk & \mu & 0 \\ 0 & 0 & \mu_o \end{bmatrix} \tag{1}$$

$$\mu = \mu_o \frac{\gamma^2 \mu_o H_o B_o - \omega^2}{\gamma^2 \mu_o^2 H_o^2 - \omega^2} \qquad k = \frac{\omega \gamma \mu_o M_o}{\gamma^2 \mu_o^2 H_o^2 - \omega^2}$$

where

$$B_o = \mu_o (H_o + M_o)$$

γ = gyromagnetic ratio of the electron in orbital motion.

$$\vec{B} = [\mu]\vec{H} \tag{2}$$

where $\vec{B}$ is magnetic flux density vector in the ferrite.

Consider Maxwell's equations:

$$\nabla \cdot \vec{\mathcal{H}} = \frac{\partial \vec{D}}{\partial t} \tag{3}$$

$$\nabla \cdot \vec{\mathcal{E}} = -\frac{\partial \vec{B}}{\partial t} \tag{4}$$

$$\nabla \cdot \vec{B} = 0 \tag{5}$$

$$\nabla \cdot \vec{\mathcal{D}} = 0 \tag{6}$$

$$\vec{B} = \mu \vec{\mathcal{H}} \tag{7}$$

$$\vec{\mathcal{D}} = \epsilon \vec{\mathcal{E}} \tag{8}$$

where

$\vec{\mathcal{E}}$: electric field vector.

$\vec{\mathcal{D}}$: electric flux density vector.

$\vec{\mathcal{H}}$: magnetic field vector.

ϵ : dielectric constant.

μ : permeability.

$\vec{B}$: magnetic flux density vector.

We neglect the conduction current source and space current source. The four vector quantities above are varying sinusoidally with time, we can re-write eqs. (3), (4) as follows:

$$\nabla x \vec{H} = j\omega\epsilon \vec{E} \tag{9}$$

$$\nabla x \vec{E} = -j\omega\vec{B} \tag{10}$$

Because of the physical arrangement, there is no variation in z-direction and $E_p = E_\phi = H_z = 0$. $\vec{E} = \vec{z}\, Ez$
From (10), we get

$$\vec{H} = j\frac{1}{\omega}\cdot\frac{1}{[\mu]}\nabla x \vec{E} \tag{11}$$

Take the curl of (11)

$$\nabla x \vec{H} = j\frac{1}{\omega}\nabla x \frac{1}{[\mu]}\nabla x \vec{E} \tag{12}$$

The left side of eq. (12) can be replaced by eq. (9), so

$$j\omega\epsilon \vec{E} = j\frac{1}{\omega}\nabla x \frac{1}{[\mu]}\nabla x \vec{E} \tag{13}$$

We let $\vec{E} = \vec{z}\, f$ in eq. (13). By working out explicitly the right side of eq. (13) and equating the z component of $\vec{E}$, we get

$$-\frac{1}{\mu^2 - k^2}\left\{\frac{1}{\rho}\frac{\partial}{\partial\rho}\left(\rho\mu\frac{\partial f}{\partial\rho}\right) - \frac{\mu}{\rho}\frac{\partial^2 f}{\partial\phi^2}\right\} = \omega^2\epsilon\, f. \tag{14}$$

The left side is ∇^2 in cylindrical coordinates, so

$$\nabla^2 f = \omega^2\epsilon\frac{\mu^2 - k^2}{\mu} f = \omega^2\epsilon\,\mu_{eff} f = \beta_f^2 f. \tag{15}$$

Consider a primary source and the ferrite post as shown in Fig. 5.

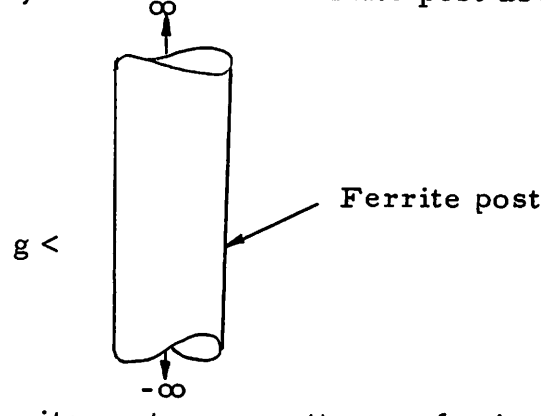

Fig. 5 Ferrite post as a scatterer of primary source g.

We put a conducting sheet over the surface of the ferrite post and remove the ferrite. The field outside the conductor is designated by $\vec{E}_{g1}$

$$\vec{E}_{g1} = \vec{E}_{go} + \vec{E}_{co} \tag{16}$$

where $\vec{E}_{go}$ is the field due to the primary source in free space.

$\vec{E}_{co}$ is the field due to the equivalent source over the place of the conductor surface.

We put the ferrite post inside the conducting sheet. The field $\vec{E}_{g1}$ will not be disturbed. $\vec{E}_{g1}$ can be expressed by

$$\vec{E}_{g1} = \vec{E}_{g2} + \vec{E}_{c2} \tag{17}$$

where $\vec{E}_{g2}$ is the field due to the primary source in the presence of the ferrite post

$\vec{E}_{c2}$ is the field due to the equivalent source in the presence of the ferrite post.

Equating (16) and (17), we have

$$\vec{E}_{go} + \vec{E}_{co} = \vec{E}_{g2} + \vec{E}_{c2} \tag{18}$$

We use any test source t to measure the fields, then

$$\langle g, t \rangle_2 - \langle g, t \rangle_0 = \langle c, t \rangle_0 - \langle c, t \rangle_2 \tag{19}$$

The explanation of the reaction formulae is given as follows: (The field due to source g at t in the presence of the ferrite post) - (the field due to the source g at t in free space) = (the field due to the equivalent source at t in free space) - (the field due to the equivalent source at t in the presence of the ferrite post) = The scattered field.

The equivalent source can be expanded into mode source m.

$$J_c = \Sigma A_m m. \tag{20}$$

By using the reciprocity theorem, the reaction $\langle c, t \rangle_0$ can be written

$$\langle c, t \rangle_0 = \langle t, c \rangle_0 = \Sigma A_m \langle t, m \rangle_0 \tag{21}$$

Let t be any one of the mode sources, m, the orthogonality condition gives A_m

$$A_m = \frac{\langle c, m \rangle_0}{\langle m, m \rangle_0} \tag{22}$$

If we move the test source to the surface of the conducting sheet, the field over the surface is zero. This means the field due to the equivalent source at the surface of the metal sheet is the negative of the field due to the primary source at the surface. The expression for A_m can be rewritten as

$$A_m = -\frac{\langle m, g\rangle_0}{\langle m,m\rangle_0} \tag{23}$$

To evaluate the reaction $\langle c, t\rangle_2$, we have to use the reciprocity theorem for the anisotropic medium, so

$$\langle c, t\rangle_2 = \langle \tilde{t}, c\rangle_2 \tag{24}$$

where $\tilde{t}$ is the field due to test source in the transposed medium at source C. Source C is the same in both cases. $\langle \tilde{t}, c\rangle_2$ can be expressed as

$$\langle \tilde{t}, c\rangle_2 = -\Sigma \frac{\langle m,g\rangle_0}{\langle m,m\rangle_0}\langle \tilde{t}, m\rangle_2 = -\Sigma \frac{\langle m,g\rangle_0}{\langle m,m\rangle_0}\langle m\, t\rangle_2 \tag{25}$$

In order to calculate $\langle m,t\rangle_2$, we consider the reaction

$$\langle m,g\rangle_2 = \langle \tilde{g}, m\rangle_2 \tag{26}$$

Recall the reaction $\langle \tilde{g}, m\rangle_2$ which is the field due to the primary source in the transposed medium at the mode source m. This field is the negative of the field due to the equivalent source in the transposed medium at the mode source m. So

$$\langle \tilde{g}, m\rangle_2 = -\langle \tilde{c}, m\rangle_2 = -\langle m, c\rangle_2 = \frac{\langle m,g\rangle_0}{\langle m,m\rangle_0}\langle m,m\rangle_2 \tag{27}$$

Because g is any primary source, we can set it to be any test source t,

$$\langle m, t\rangle_2 = \frac{\langle m, t\rangle_0}{\langle m,m\rangle_0}\langle m, m\rangle_2 \tag{28}$$

From eqs. (19), (21), (23), (24), (25) and (28), the scattered field can be obtained

$$\langle g, t\rangle_2 - \langle g, t\rangle_0 = \Sigma\left\{\frac{\langle m,m\rangle_2}{\langle m,m\rangle_0} - 1\right\}\frac{\langle m,g\rangle_0}{\langle m,m\rangle_0}\langle m,t\rangle_0 \tag{29}$$

For the calculations of $\langle m,m \rangle_2$ and $\langle m,m \rangle_0$, the mode source can be obtained by finding the discontinuity of the tangential component of $\vec{H}$ at the surface of the boundary.

A. In the Presence of the Ferrite Post

By working out eq. (9) explicitly, we equate the $\vec{\rho}$ and $\vec{\phi}$ components,

$$j\omega\mu H_\rho + \omega k H_\phi = -\frac{1}{\rho}\frac{\partial f}{\partial \phi} \tag{30}$$

$$-\omega k H_\rho + j\omega\mu H_\phi = \frac{\partial f}{\partial \rho} \tag{31}$$

solving H_ρ and H_ϕ, we get

$$H_\phi = \frac{1}{\omega(\mu^2 - k^2)}\left\{-j\mu\frac{\partial f}{\partial \rho} + \frac{k}{\rho}\frac{\partial f}{\partial \phi}\right\} \tag{32}$$

$$H_\rho = \frac{1}{\omega(\mu^2 - k^2)}\left\{j\frac{\mu}{\rho}\frac{\partial f}{\partial \phi} + k\frac{\partial f}{\partial \rho}\right\} \tag{33}$$

Outside the ferrite medium, the component H_ϕ is simply given by

$$H_\phi = \frac{1}{j\omega\mu_o}\frac{\partial f}{\partial \rho} \tag{34}$$

The mode fields f are as follows:

$$\rho > a \qquad f_o = E_{z20} = \Sigma A_n H_n^{(2)}(\beta_o \rho) e^{-jn\phi} \qquad \beta_o = \omega\sqrt{\mu_o \epsilon_o} \tag{35}$$

$$\rho < a \qquad f_i = E_{z2i} = \Sigma F_n J_n(\beta_\phi \rho) e^{-jn\phi} \tag{36}$$

At $\rho = a$, E_z is continuous,

$$A_n H_n^{(2)}(\beta_o a) = F_n J_n(\beta_f a). \tag{37}$$

The mode source J_{c2} is

$$J_{c2} = jA_n\left[-\frac{\beta_o}{\omega\mu_o}H_n^{(2)}(\beta_o a) + \frac{H_n^{(2)}(\beta_o a)}{\omega(\mu^2 - k^2)J_n(\beta_f a)}\right.$$

$$\left.\left\{\beta_f \mu J_n'(\beta_f a) + \frac{kn}{a}J_n(\beta_f a)\right\}\right] e^{-jn\phi} \tag{38}$$

B. In Free Space

The mode fields are designated by g,

$$\rho > a \qquad g_o = E_{z00} = \Sigma C_n H_n^{(2)} (\beta_o \rho)\, e^{-jn\phi} \tag{39}$$

$$\rho < a \qquad g_i = E_{z0i} = \Sigma D_n J_n (\beta_o \rho)\, e^{-jn\phi} \tag{40}$$

The tangential components of H_ϕ are given by

$$\rho > a \qquad H_{\phi 0} = \frac{\beta_o}{j\omega\mu_o} C_n H_n^{(2)'} (\beta_o \rho)\, e^{-jn\phi} \tag{41}$$

$$\rho < a \qquad H_{\phi i} = \frac{\beta_o}{j\omega\mu_o} D_n J_n (\beta_o \rho)\, e^{-jn\phi} \tag{42}$$

At $\rho = a$, E_{z0} is continuous.

The relation between two undetermined coefficients is

$$C_n H_n^{(2)} (\beta_o a) = D_n J_n (\beta_o a) \tag{43}$$

The mode source is expressed as

$$J_{c0} = \frac{\beta_o C_n}{j\omega\mu_o} \left\{ H_n^{(2)'} (\beta_o a) - \frac{H_n^{(2)} (\beta_o a)}{J_n (\beta_o a)} J_n' (\beta_o a) \right\} e^{-jn\phi} \tag{44}$$

In these two cases, the mode sources are same, i. e.,

$$J_{c2} = J_{c0} \tag{45}$$

The reactions of $\langle m, m \rangle_2$ and $\langle m, m \rangle_0$ are calculated as follows

$$\langle m\, m \rangle_2 = \int J_{m2} E_{m2} ds = \lim_{z \to \infty} \int_{-z}^{z} dz \int_0^{2\pi} jA_n^2 H_n^{(2)} (\beta_o a)$$

$$\left[-\frac{\beta_o}{\omega\mu_o} H_n^{(2)'} (\beta_o a) + \frac{H_n^{(2)} (\beta_o a)}{\omega(\mu^2 - k^2) J_n (\beta_f a)} \left\{ \mu\beta_f J_n' (\beta_f a) + \frac{kn}{a} J_n (\beta_f a) \right\} \right]$$

$$\cdot\, e^{-j2n\phi} a \cdot d\phi \tag{46}$$

$$\langle m\,m\rangle_0 = \int J_{m0}E_{m0}ds = \lim_{z\to\infty}\int_{-z}^{z}dz\int_0^{2\pi}(-j)C_n^2H_n^{(2)}(\beta_o a)\frac{1}{\omega\mu_o}$$

$$\left\{H_n^{(2)'}(\beta_o a) - \frac{H_n^{(2)}(\beta_o a)}{J_n(\beta_o a)}J_n'(\beta_o a)\right\}e^{-2jn\phi}\cdot a\,d\phi \tag{47}$$

Then

$$\langle g,t\rangle_2 - \langle g,t\rangle_0 = \Sigma\left\{\frac{\left\{-\frac{\beta_o}{\mu_o}\left\{H_n^{(2)'}(\beta_o a) - \frac{H_n^{(2)}(\beta_o a)}{J_n(\beta_o a)}J_n'(\beta_o a)\right\} + \frac{\beta_o}{\mu_o}H_n^{(2)'}(\beta_o a) - \frac{H_n^{(2)}(\beta_o a)}{(\mu^2-k^2)J_n(\beta_f a)}\left[\mu\beta_f J_n'\beta_f a) + \frac{kn}{a}J_n(\beta_f a)\right]\right\}}{-\frac{\beta_o}{\mu_o}H_n^{(2)'}(\beta_o a) + \frac{H_n^{(2)}(\beta_o a)}{(\mu^2-k^2)J_n(\beta_f a)}\left[\mu\beta_f J_n'(\beta_f a) + \frac{kn}{a}J_n(\beta_f a)\right]}\right\}$$

$$\cdot\frac{\langle g,m\rangle_0}{\langle m,m\rangle_0}\langle m,t\rangle_0 \tag{48}$$

If we know the field due to the primary source as in this case,

$$E_{g0} = \Sigma(j)^n E_o J_n(\beta_o\rho)e^{-jn\phi} \tag{49}$$

The reaction $\langle g,m\rangle_0$ is

$$\langle g\,m\rangle_0 = \lim_{z\to\infty}\int_{-z}^{z}dz\int_0^{2\pi}(-j)(j)^n E_o J_n(\beta_a)\frac{\beta_o C_n}{\omega\mu_o}\left[H_n^{(2)'}(\beta_o a) - \frac{H_n^{(2)}(\beta_o a)}{J_n(\beta_o a)}J_n'(\beta_o a)\right]e^{-j2n\phi}a\,d\phi \tag{50}$$

Finally, the scattered field is

$$\langle g\,t\rangle_2 - \langle g\,t\rangle_0 = E_{z\,s} = \Sigma(j)^n E_o \left\{ \frac{\left\{ \frac{\beta_o}{\mu_o} J_n'(\beta_o a) J_n(\beta_f a) - \frac{J_n'(\beta_o a)}{(\mu^2 - k^2)} \left\{ \mu\beta_f J_n'(\beta_f a) + \frac{kn}{a} J_n(\beta_f a) \right\} \right\}}{\frac{H_n^{(2)}(\beta_o a)}{(\mu^2 - k^2)} \left\{ \mu\beta_f J_n'(\beta_f a) + \frac{kn}{a} J_n(\beta_f a) \right\} - \frac{\beta_o}{\mu_o} H_n^{(2)'}(\beta_o a) J_n(\beta_f a)} \right\} \cdot H_n^{(2)}(\beta_o \rho) e^{-jn\phi} \tag{51}$$

The corresponding $H_{\phi s}$ and $H_{\rho s}$ are given by

$$H_{\phi s} = -\Sigma(j)^{n+1} E_o \frac{\beta_o}{\omega\mu_o} \left\{ \frac{\frac{\beta_o}{\mu_o} J_n'(\beta_o a) J_n(\beta_f a) - \frac{J_n(\beta_o a)}{(\mu^2 - k^2)} \left[\mu\beta_f J_n'(\beta_f a) + \frac{nk}{a} J_n(\beta_f a) \right]}{\frac{H_n^{(2)}(\beta_o a)}{(\mu^2 - k^2)} \left[\mu\beta_f J_n'(\beta_f a) + \frac{nk}{a} J_n(\beta_f a) \right] - \frac{\beta_o}{\mu_o} J_n(\beta_f a) H_n^{(2)'}(\beta_o a)} \right\} \cdot H_n^{(2)'}(\beta_o \rho) e^{-jn\phi} \tag{52}$$

$$H_{\rho s} = \frac{1}{\omega\mu_o \rho} \Sigma(j)^n E_o \left\{ \frac{\frac{\beta_o}{\mu_o} J_n'(\beta_o a) J_n(\beta_f a) - \frac{J_n(\beta_o a)}{(\mu^2 - k^2)} \left[\mu\beta_f J_n'(\beta_f a) + \frac{nk}{a} J_n(\beta_f a) \right]}{\frac{H_n^{(2)}(\beta_o a)}{(\mu^2 - k^2)} \left[\mu\beta_f J_n'(\beta_f a) + \frac{nk}{a} J_n(\beta_f a) \right] - \frac{\beta_o}{\mu_o} J_n(\beta_f a) H_n^{(2)'}(\beta_o a)} \right\} \cdot H_n^{(2)}(\beta_o \rho) \cdot e^{-jn\phi} \tag{53}$$

From eqs. (51), (52) and (53), the scattered field is TE mode. Using the recurrence formula for Bessel's function,

$$H_n^{(2)'}(\beta_o\rho) = \frac{n}{\beta_o\rho} H_n^{(2)}(\beta_o\rho) - H_{n+1}^{(2)}(\beta_o\rho)$$

$$J_n'(\beta\rho) = \frac{n}{\beta\rho} J_n(\beta\rho) - J_{n+1}(\beta\rho) \tag{54}$$

the magnetic field vector is elliptically polarized for small ρ. For large ρ, H_ρ dies out. The scattered field becomes a TEM field. The asymptotic expansion of $H_n^{(2)}(\beta_o\rho)$ for large $(\beta_o\rho)$ is

$$H_n^{(2)}(\beta_o\rho) \longrightarrow (j)^n\sqrt{\frac{2}{\pi\beta_o\rho}}\; e^{-j\left[\beta_o\rho-\frac{\pi}{4}\right]} = (j)^n H_o^{(2)}(\beta_o\rho). \tag{55}$$

$$E_{zs} = -E_o\Sigma(-1)^n \frac{\frac{\beta_f}{\beta_o}\frac{J_{n+1}(\beta_f a)}{J_n(\beta_f a)} + \frac{J_{n+1}(\beta_o a)}{J_n(\beta_o a)}}{\frac{\beta_f}{\beta_o}\frac{J_{n+1}(\beta_f a)}{J_n(\beta_f a)} + \frac{H_{n+1}^{(2)}(\beta_o a)}{H_n^{(2)}(\beta_o a)}} \times \frac{J_n(\beta_o a)}{H_n^{(2)}(\beta_o a)}\sqrt{\frac{2}{\pi\beta_o\rho}}$$
$$\cdot e^{-j\left[\beta_o\rho-\frac{\pi}{4}\right]} \cdot e^{-jn\phi} \tag{56}$$

If $H_o = 0$, $\mu = \mu_o$, $k = 0$, $\beta_f = \sqrt{\epsilon}\,\beta_o$ then

$$E_{zs} = -E_o\left\{\frac{\frac{\beta_f}{\beta_o}\frac{J_1(\beta_f a)}{J_o(\beta_f a)} + \frac{J_1(\beta_o a)}{J_o(\beta_o a)}}{\frac{\beta_f}{\beta_o}\frac{J_1(\beta_f a)}{J_o(\beta_f a)} + \frac{H_1^{(2)}(\beta_o a)}{H_o^{(2)}(\beta_o a)}} \frac{J_o(\beta_o a)}{H_o^{(2)}(\beta_o a)} + \Sigma 2(-1)^n \frac{\frac{\beta_f}{\beta_o}\frac{J_{n+1}(\beta_f a)}{J_n(\beta_f a)} + \frac{J_{n+1}(\beta_o a)}{J_n(\beta_o a)}}{\frac{\beta_f}{\beta_o}\frac{J_{n+1}(\beta_f a)}{J_n(\beta_f a)} + \frac{H_{n+1}^{(2)}(\beta_o a)}{H_n^{(2)}(\beta_o a)}}\right.$$
$$\left. \times \frac{J_n(\beta_o a)}{H_n^{(2)}(\beta_o a)} \cos n\phi \right\} \tag{57}$$

In eq. (57) $\cos n\phi$ is an even function. This shows the pattern is symmetric with respect to $\phi = 0$.

When we reverse the d-c magnetic field, we set a new coordinate system X', Y', Z', with Z' in the direction of $\vec{H}_o$. The relation between the coordinate systems is shown in Fig. 6.

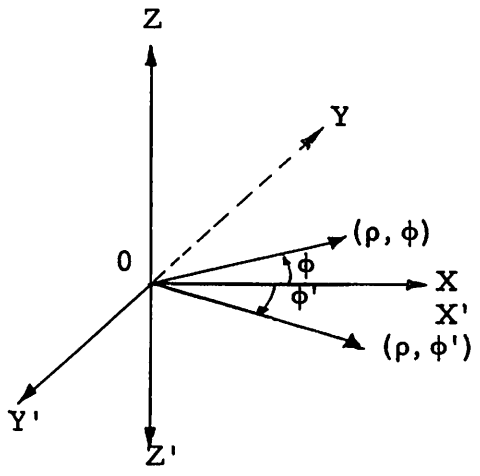

Fig. 6 The relation of coordinate systems for both directions of d-c magnetic field.

In this new coordinate system, ϕ' varies in opposite direction as ϕ. The incident wave is now polarized in the -Z' direction; this yields the reaction $\langle gm \rangle_0$ to be negative. The scattered field in the new coordinate system is

$$E_{zs} = -\Sigma (j)^n E_o \frac{\frac{\beta_o}{\mu_o} J_n'(\beta_o a) J_n(\beta_f a) - \frac{J_n(\beta_o a)}{(\mu^2 - k^2)} \left\{ \mu \beta_f J_n'(\beta_f a) + \frac{kn}{a} J_n(\beta_f a) \right\}}{\frac{H_n^{(2)}(\beta_o a)}{(\mu^2 - k^2)} \left\{ \mu \beta_f J_n'(\beta_f a) + \frac{kn}{a} J_n(\beta_f a) \right\} - \frac{\beta_o}{\mu_o} H_n^{(2)'}(\beta_o a) J_n(\beta_f a)}$$

$$\cdot H_n^{(2)}(\beta_o \rho) \cdot e^{-jn\phi'} \qquad (58)$$

Comparing to the case before, the constant part except the negative sign and the variation in ρ are the same in both cases. The scattered field is a mirror image as we reverse the d-c magnetic field.

Comparing to eqs. (51) and (35), the coefficient A_n is

$$A_n = (j)^n E_o \frac{\frac{\beta_o}{\mu_o} J_n'(\beta_o a) J_n(\beta_f a) - \frac{J_n(\beta_o a)}{(\mu^2 - k^2)} \left\{ \mu \beta_f J_n'(\beta_f a) + \frac{kn}{a} J_n(\beta_f a) \right\}}{\frac{H_n^{(2)}(\beta_o a)}{(\mu^2 - k^2)} \left\{ \mu \beta_f J_n'(\beta_f a) + \frac{kn}{a} J_n(\beta_f a) \right\} - \frac{\beta_o}{\mu_o} H_n^{(2)'}(\beta_o a) J_n(\beta_f a)} \qquad (59)$$

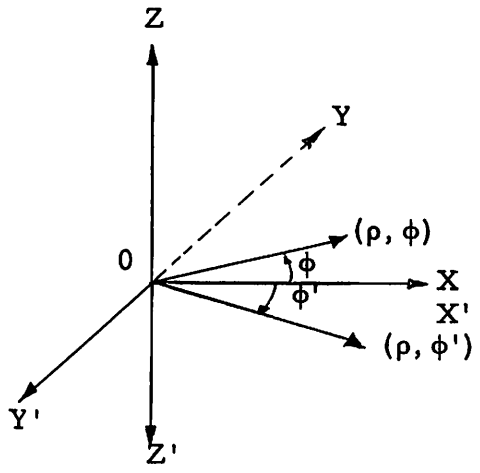

Fig. 6 The relation of coordinate systems for both directions of d-c magnetic field.

In this new coordinate system, ϕ' varies in opposite direction as ϕ. The incident wave is now polarized in the -Z' direction; this yields the reaction $\langle gm \rangle_0$ to be negative. The scattered field in the new coordinate system is

$$E_{zs} = -\Sigma (j)^n E_o \frac{\frac{\beta_o}{\mu_o} J_n'(\beta_o a) J_n(\beta_f a) - \frac{J_n(\beta_o a)}{(\mu^2 - k^2)} \left\{ \mu \beta_f J_n'(\beta_f a) + \frac{kn}{a} J_n(\beta_f a) \right\}}{\frac{H_n^{(2)}(\beta_o a)}{(\mu^2 - k^2)} \left\{ \mu \beta_f J_n'(\beta_f a) + \frac{kn}{a} J_n(\beta_f a) \right\} - \frac{\beta_o}{\mu_o} H_n^{(2)'}(\beta_o a) J_n(\beta_f a)}$$

$$\cdot H_n^{(2)}(\beta_o \rho) \cdot e^{-jn\phi'} \qquad (58)$$

Comparing to the case before, the constant part except the negative sign and the variation in ρ are the same in both cases. The scattered field is a mirror image as we reverse the d-c magnetic field.

Comparing to eqs. (51) and (35), the coefficient A_n is

$$A_n = (j)^n E_o \frac{\frac{\beta_o}{\mu_o} J_n'(\beta_o a) J_n(\beta_f a) - \frac{J_n(\beta_o a)}{(\mu^2 - k^2)} \left\{ \mu \beta_f J_n'(\beta_f a) + \frac{kn}{a} J_n(\beta_f a) \right\}}{\frac{H_n^{(2)}(\beta_o a)}{(\mu^2 - k^2)} \left\{ \mu \beta_f J_n'(\beta_f a) + \frac{kn}{a} J_n(\beta_f a) \right\} - \frac{\beta_o}{\mu_o} H_n^{(2)'}(\beta_o a) J_n(\beta_f a)} \qquad (59)$$

At $\rho = a$, with the incident plane wave, we have

$$F_n J_n(\beta_f a) = A_n H_n^{(2)}(\beta_o a) + (j)^n E_o J_n(\beta_o a) \tag{60}$$

From eq. (60), the coefficient F_n can be evaluated,

$$F_n = \frac{(j)^{n+1} 2E_o}{\mu_o \pi a \left[\frac{H_n^{(2)}(\beta_o a)}{(\mu^2 - k^2)} \left\{ \mu \beta_f J_n'(\beta_f a) + \frac{kn}{a} J_n(\beta_f a) \right\} - \frac{\beta_o}{\mu_o} H_n^{(2)'}(\beta_o a) J_n(\beta_f a) \right]} \tag{61}$$

The field inside the ferrite is given as follows:

$$E_{zi} = \sum_n \frac{(j)^{n+1}}{\mu_o \pi a} \frac{2E_o}{\frac{H_n^{(2)}(\beta_o a)}{(\mu^2 - k^2)} \left\{ \mu \beta_f J_n'(\beta_f a) + \frac{kn}{a} J_n(\beta_f a) \right\} - \frac{\beta_o}{\mu_o} H_n^{(2)'}(\beta_o a) J_n(\beta_f a)} J_n(\beta_f \rho) e^{-jn\phi} \tag{62}$$

$$H_{\phi i} = -\sum_n \frac{(j)^{n+2}}{\pi a \mu_o \omega (\mu^2 - k^2)} \frac{2E_o \left\{ \mu \beta_f J_n'(\beta_f a) - \frac{nk}{\rho} J_n(\beta_f a) \right\}}{\frac{H_n^{(2)}(\beta_o a)}{(\mu^2 - k^2)} \left\{ \mu \beta_f J_n'(\beta_f a) + \frac{kn}{a} J_n(\beta_f a) \right\} - \frac{\beta_o}{\mu_o} H_n^{(2)'}(\beta_o a) J_n(\beta_f a)} e^{-jn\phi} \tag{63}$$

$$H_{\rho i} = \sum_n \frac{(j)^{n+1}}{\pi a \mu_o \omega (\mu^2 - k^2)} \frac{2E_o \left\{ \frac{\mu n}{\rho} J_n(\beta_f a) + k \beta_f J_n'(\beta_f a) \right\}}{\frac{H_n^{(2)}(\beta_o a)}{(\mu^2 - k^2)} \left\{ \mu \beta_f J_n'(\beta_f a) + \frac{kn}{a} J_n(\beta_f a) \right\} - \frac{\beta_o}{\mu_o} H_n^{(2)'}(\beta_o a) J_n(\beta_f a)} e^{-jn\phi} \tag{64}$$

The results show the field inside the ferrite is TE mode, and the magnetic field is elliptically polarized.

From eq. (59), we rewrite A_n as follows:

$$A_{\pm n} = j^n \left\{ \frac{\frac{\epsilon_f}{\epsilon_o}\cdot\frac{\beta_o}{\beta_f}\left[\frac{n}{\beta_f a}\left(1\pm\frac{k}{\mu}\right) - \frac{J_{n+1}(\beta_f a)}{J_n(\beta_f a)} - \frac{n}{\beta_o a} + \frac{J_{n+1}(\beta_o a)}{J_n(\beta_o a)}\right]}{\frac{\epsilon_f}{\epsilon_o}\frac{\beta_o}{\beta_f}\left[\frac{n}{\beta_f a}\left(1\pm\frac{k}{\mu}\right) - \frac{J_{n+1}(\beta_f a)}{J_n(\beta_f a)} - \frac{n}{\beta_o a} + \frac{H_{n+1}^{(2)}(\beta_o a)}{H_n^{(2)}(\beta_o a)}\right]} \right\} \cdot \frac{J_n(\beta_o a)}{H_n^{(2)}(\beta_o a)} E_o \tag{65}$$

Combining eqs. (65) and (55), E_{zso} can be expressed as

$$E_{zso} = j H_o^{(2)}(\beta_o \rho) \left\{ A_o + \sum_1^{\infty} \left[(-1)^n (A'_{-n} + A'_n)\cos n\phi + j(A'_{-n} - A'_n)\sin n\phi \right] \right\} E_o \tag{66}$$

where $A'_{\pm n} = -(j)^{-n} A_{\pm n}$.

The phase angle of the scattered field is

$$\tan\theta = \frac{\sum_1^{\infty} (-1)^n \cdot (A'_{-n} - A'_n)\sin n\phi}{A_o + \sum_1^{\infty} (-1)^n (A'_{-n} + A'_n)\cos n\phi} \tag{67}$$

For $\beta_f a$ and $\beta_o a$ very small, the approximate expressions of the Bessel's functions are

$$J_n(\beta a) = \frac{(\beta a)^n}{n!\,2^n} \tag{68}$$

$$H_n^{(2)}(\beta a) = \frac{(n-1)!}{\pi}\left(\frac{2}{\beta a}\right)^n \tag{69}$$

We only take n = 0, 1, -1.

$$A_o = j\frac{\pi}{4}(\beta_o a)^2 \left(\frac{\epsilon_f}{\epsilon_o} - 1\right) E_o \tag{70}$$

$$A_1' = -jE_o \frac{\frac{\mu_o}{\mu_{eff}}(1+\frac{k}{\mu})-1}{(\frac{\mu_o}{\mu_{eff}})(1+\frac{k}{\mu})+1} \cdot \frac{\pi}{4} \cdot (\beta_o a)^2 \tag{71}$$

$$A_{-1}' = -jE_o \frac{\frac{\mu_o}{\mu_{eff}}(1-\frac{k}{\mu})-1}{(\frac{\mu_o}{\mu_{eff}})(1-\frac{k}{\mu})+1} \cdot \frac{\pi}{4} \cdot (\beta_o a)^2 \tag{72}$$

The value of tan θ can be approximated as

$$\tan\theta \doteq \frac{(\frac{\mu_o}{\mu_{eff}}) \cdot \frac{k}{\mu} \sin\phi}{\left[(\frac{\mu_o}{\mu_{eff}})^2(1+\frac{k^2}{\mu^2})-1\right]\cos\theta - \frac{1}{2}(\frac{\epsilon_f}{\epsilon_o}-1)\left\{(\frac{\mu_o}{\mu_{eff}}+1)^2-(\frac{k}{\mu}\cdot\frac{\mu_o}{\mu_{eff}})^2\right\}} \tag{73}$$

If we get $\frac{\epsilon_f}{\epsilon_o} = 12$ and $\frac{\mu_o}{\mu_{eff}} = 1$, then tan θ is

$$\tan\theta \doteq \frac{\frac{}{\mu}\sin\phi}{(\frac{k}{\mu})^2\cos\phi + 5.5(\frac{k}{\mu})^2 - 22} \tag{74}$$

The curves for $\frac{k}{\mu} = 2$, $\frac{}{\mu} = 2.5$ and $\frac{k}{\mu} = 3$ are plotted.

IV. MEASUREMENT RESULTS AND THEIR RELATION TO THE THEORY

In doing the measurement, we check the correct microwave frequency first as described in Sec. II. The pattern without putting the ferrite into the ground plates, the reaction $\langle g, t\rangle_0$ in Eq. (51), is symmetric with respect to the line joining 5-185 degrees of the angular scale on the turntable. We take this line as the axis of the transmitting antenna and call it $\phi = 0$. The

difference between this pattern and the pattern with the ferrite post in the ground plates, which gives the reaction $\langle g, t \rangle_2$ in eq. (51), is the scattered pattern.

The scattered pattern of the post without the static magnetic field applied shows that the ferrite acts as a dielectric post with dielectric constant of about 12 at frequency 9372 mc/sec., for the R-1 type ferrite. The reason is that the pattern is quite symmetric with respect to $\phi = 0$. This agrees with the solution of eq. (57).

When we apply the static magnetic field along the axis of the post (the Z-direction), the permeability of the ferrite is no longer a constant. It is expressed in eq. (1) and is called tensor permeability. The quantities μ and k are functions of H_o, where H_o is the d-c magnetic field to saturate the ferrite post. From the catalogue of the R-1 type ferrite, the value of the saturation magnetic induction is about 1750 gauss. In these measurements, the range of the d-c magnetic field is 1700-2930 gauss. Under the application of the d-c magnetic field, the gyromagnetic property of the ferrite causes the scattered pattern to be asymmetric with respect to $\phi = 0$ as predicted in eq. (56).

All the measured scattered patterns show the main lobes are deflected to one side of $\phi = 0$ (120-degree side). With the stated range of the applied d-c magnetic field, the deflections vary between 10-20 degrees from the axis. The variation of the deflection is not monotonic with the increasing of the d-c magnetic field. The maximum intensity of the main lobe occurs at 1950 gauss of the d-c magnetic field and the minimum is at 2400 gauss. The difference between the two intensities is 3.04 db.

Each pattern shows a significant side lobe occurring at the same side as the main lobe. For different d-c magnetic field the angular positions of the side lobe vary between 40-45 degrees from the axis $\phi = 0$. Compared to the intensity of the main lobe, the side lobe has its relative maximum intensity (.024 db down to the intensity of the corresponding main lobe) at 2400 gauss of the d-c magnetic field.

As we discussed in Sec. III, the scattered pattern is the mirror image of the previous case with respect to $\phi = 0$, when the d-c magnetic field is reversed (in Z' direction). This is due to the non-reciprocal property of the ferrite. The measured results quite agree with what is shown in eq. (58).

The scattered patterns, in these cases, are at the other side of $\phi = 0$ (150-degree side). Compared to the previous pattern with the same value of the d-c magnetic field, the deflection of the maximum of the main lobe occurs at the symmetric angular position with respect to the axis. The main lobe has maximum intensity at 1950 gauss of d-c magnetic field and minimum intensity at 2400 gauss. The difference between the two intensities is 2.97 db.

It is interesting to note the side lobe of each pattern is also a mirror image of the pattern with the d-c magnetic field in the Z-direction. At 2400 gauss, the side lobe has maximum relative intensity (0.03 db down to corresponding intensity of the main lobe).

From the plot of the μ and k, we get $\mu = 0$ at 2600 gauss of the static magnetic field. The patterns corresponding to $\mu = 0$, however, do not show appreciable change. The reason is that we calculate the tensor permeability without taking into account damping effects in the ferrite.

Extra measurements are taken at a d-c magnetic field of 3340 gauss, the field corresponding to a Lamor frequency of 9372 mc/sec. The deflections of the main lobe is 10-degree to $\phi = 0$. The side lobes in this case are relatively low; they are about 4 db down to the intensities of the corresponding main lobes.

In order to check the occurrence of the side lobe, we reversed the ferrite post and measured the scattered patterns with H_o in Z-and Z'-directions, respectively. The gyromagnetic property of the ferrite depends on the d-c magnetic field only. So, with the same value of H_o, the scattered patterns of the reversed ferrite post should be the same as before. The measured patterns are in good agreement to what we expect. We also notice that the maximum intensity of the main lobe occurs at 1950 gauss for both directions of the d-c magnetic field.

The side lobe appears in each scattered pattern. The angular position of the side lobe is the same with the corresponding pattern without reversing the ferrite post. These results show that the scattered pattern of the ferrite post has a significant side lobe.

For the purpose of comparison, a ferrite post with 3"/16 diameter is used as the scatterer. The scattered pattern without d-c magnetic field

applied along its axis shows also the symmetry with respect to $\phi = 0$, as predicted in eq. (56). The intensity of the main lobe is 4.96 db down to the corresponding intensity of the pattern of the 7"/8 ferrite post.

With the d-c magnetic field applied, the gyromagnetic property causes the scattered pattern to be asymmetric to $\phi = 0$. The main lobe is deflected to the 120-degree side of the axis. The deflection is 10-25 degrees. The angular positions of the side lobe are 40-50 degrees from $\phi = 0$. The minimum intensity of the main lobe occurs at 2600 gauss corresponding to the value of d-c magnetic field to give $\mu = 0$. At 3340 gauss, the deflection of the main lobe is 25 degrees from the axis and the side lobe is weak (about 5 db down to the intensity of the corresponding main lobe).

When the d-c magnetic field is in Z'-direction, the scattered patterns show clearly the non-reciprocal property of the ferrite. All the patterns are at the 150-degree side of the axis. The positions of the deflection of the lobes are the mirror images of the patterns with H_o in Z-direction.

Compared to the scattered patterns of the larger scatterer, these patterns have two special features: First, the intensity of the scattered patterns is low (about 5 db down). Secondly, the relative intensity of the side lobe (the ratio between the intensity of the corresponding main lobe and the intensity of the side lobe) is large, i.e., the scattered field of the small ferrite post has a strong side lobe.

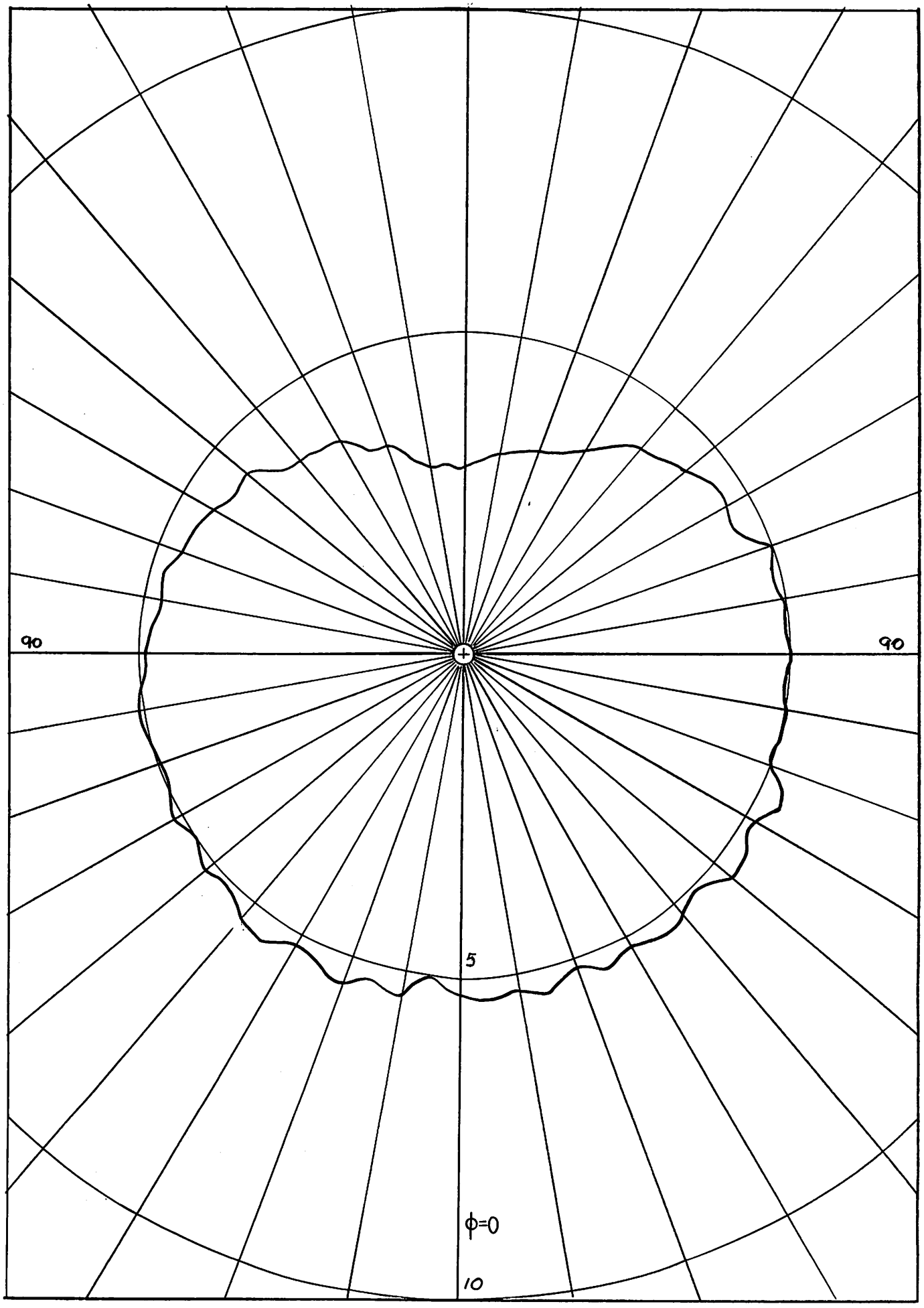

Pattern of the Transmitting Antenna in db

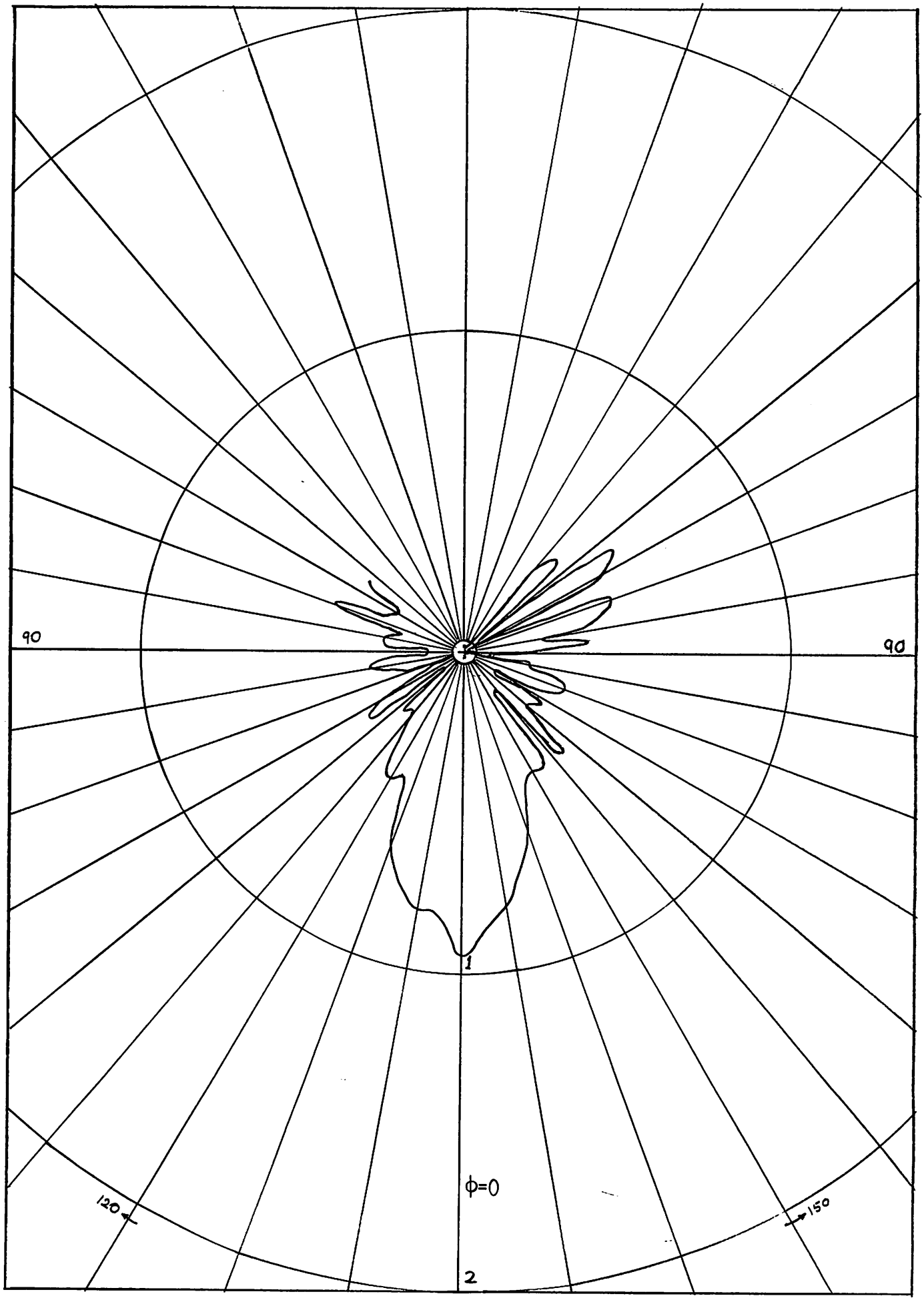

Scattered Pattern in volts 0 dc Magnetic Field
Sample = 7"/8 Ferrite Post

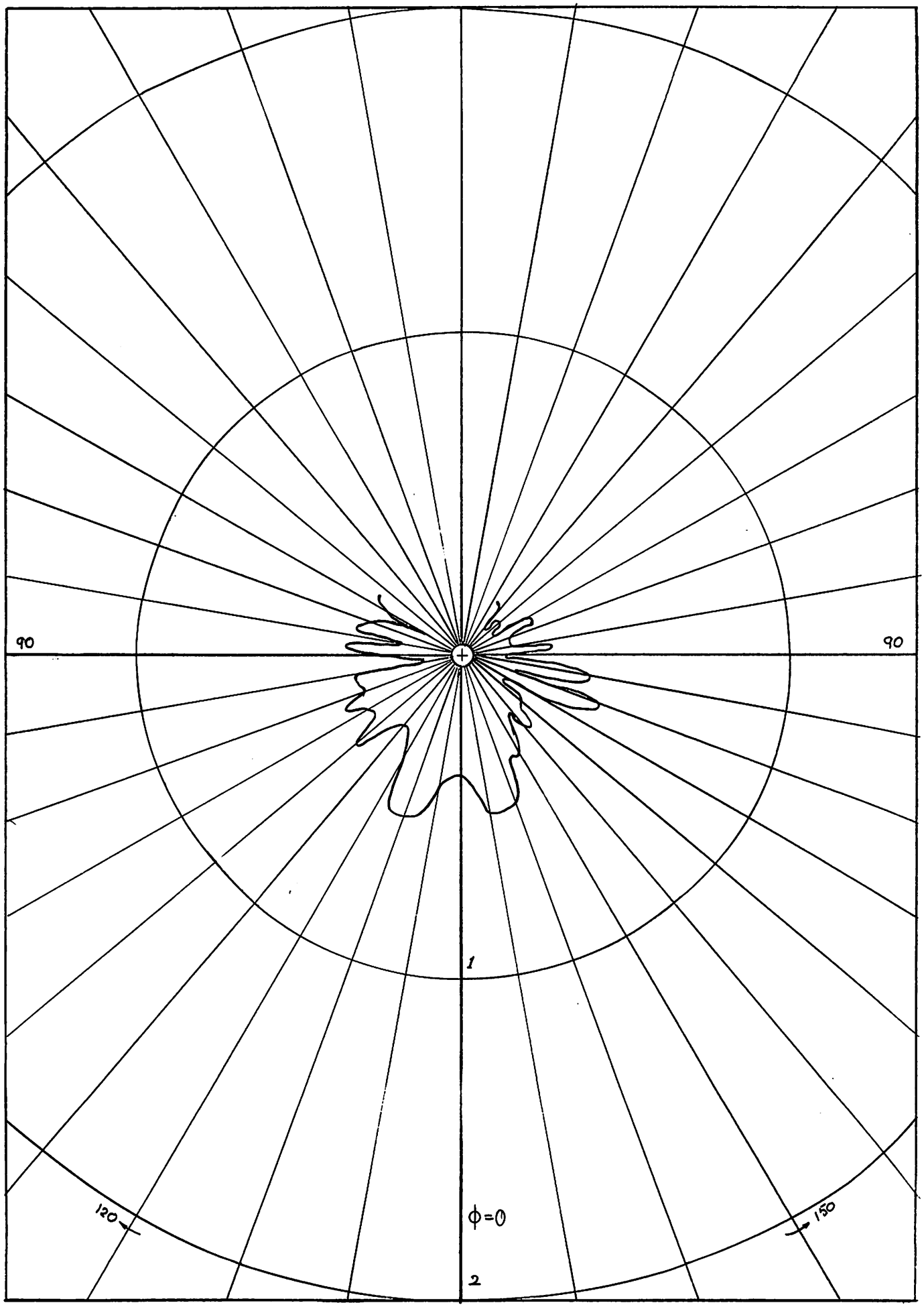

Scattered Field Pattern in volts 0 dc Magnetic Field Sample = 3"/16 Ferrite Post

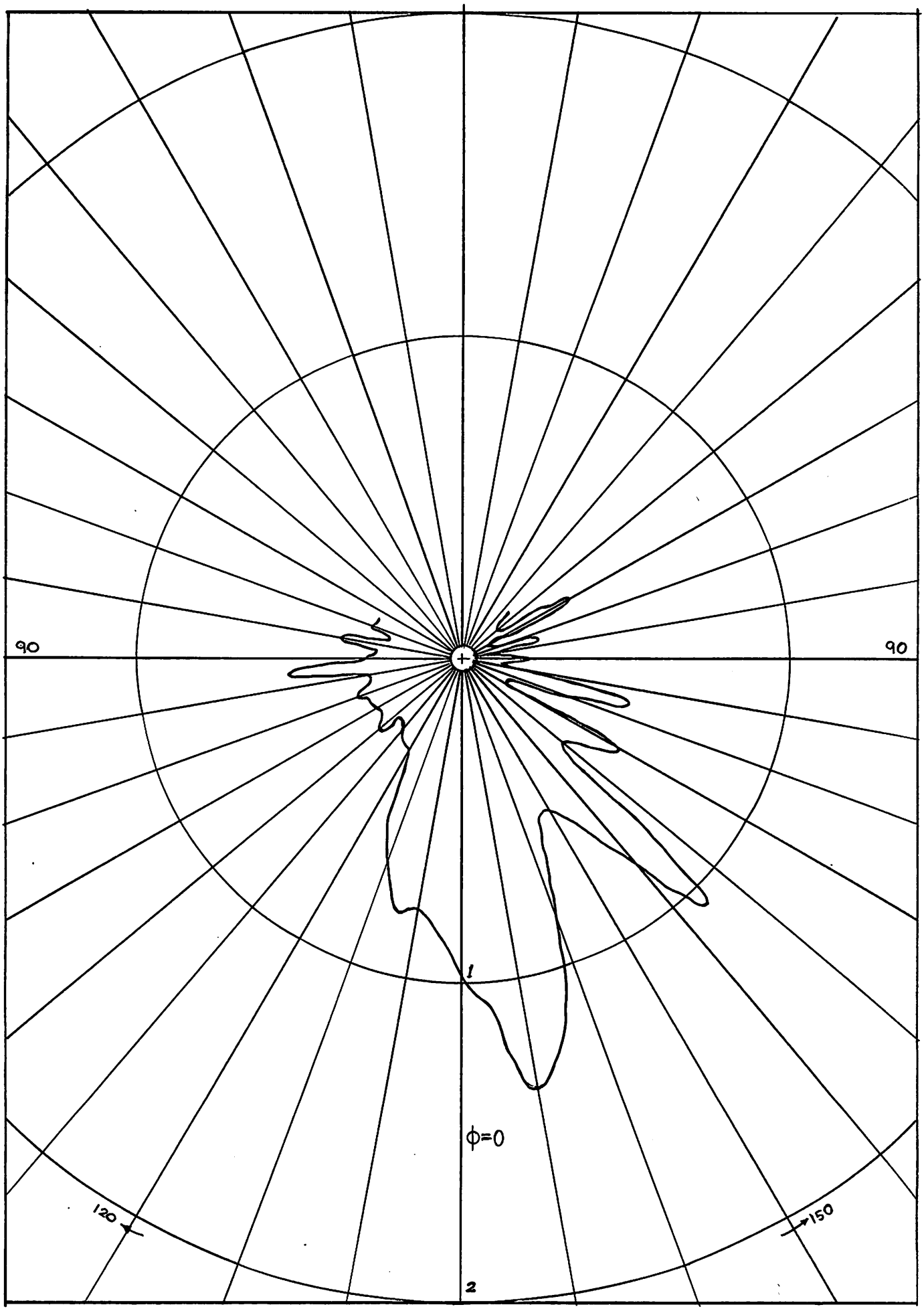

Scattered Field Pattern in Volts Ferrite Normal 1.95 kilogauss
Reversed dc Magnetic Field. Sample = 7"/8 Ferrite Post

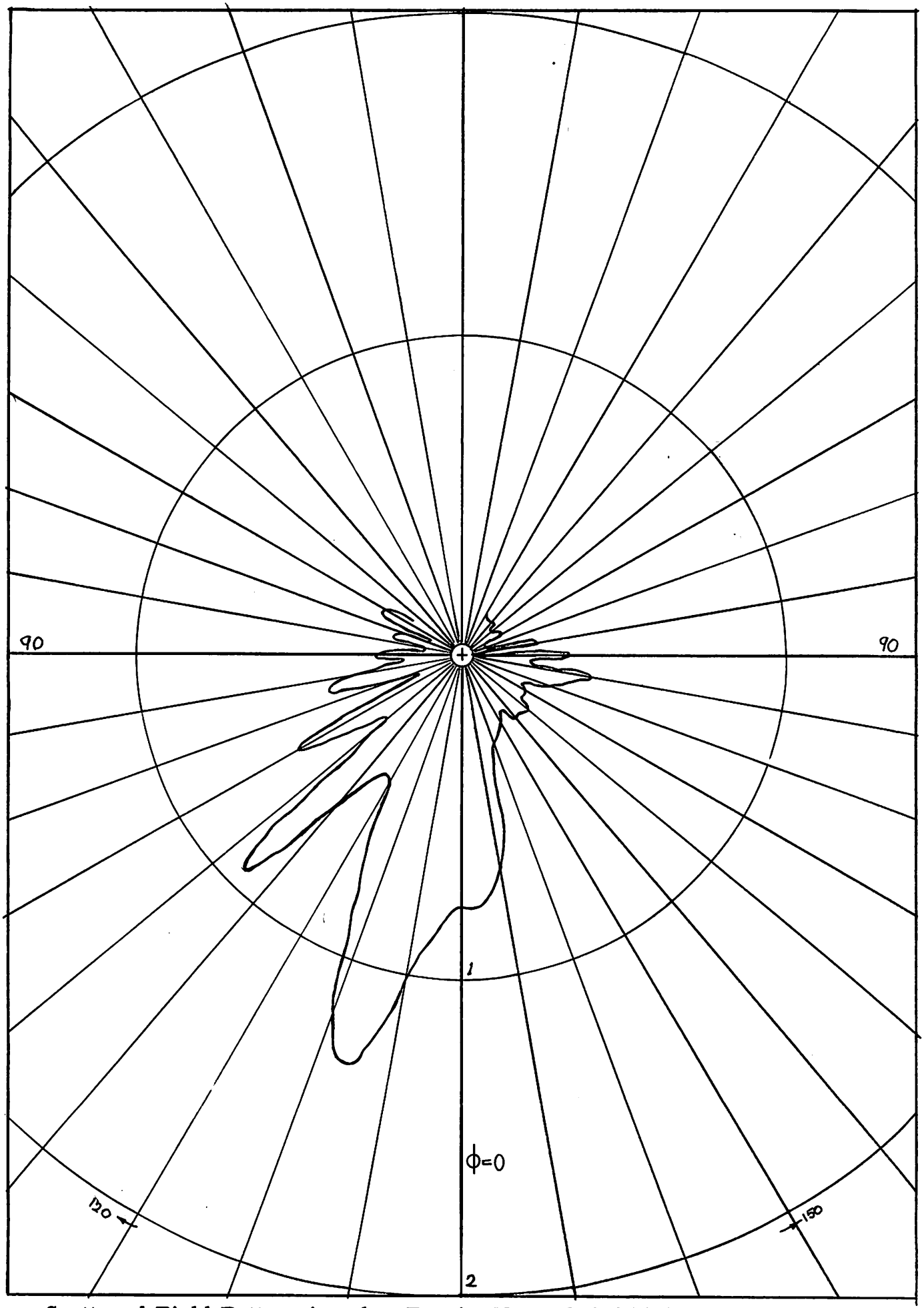

Scattered Field Pattern in volts Ferrite Normal 1. 95 kilogauss
dc Magnetic Field. Sample = 7"/8 Ferrite Post

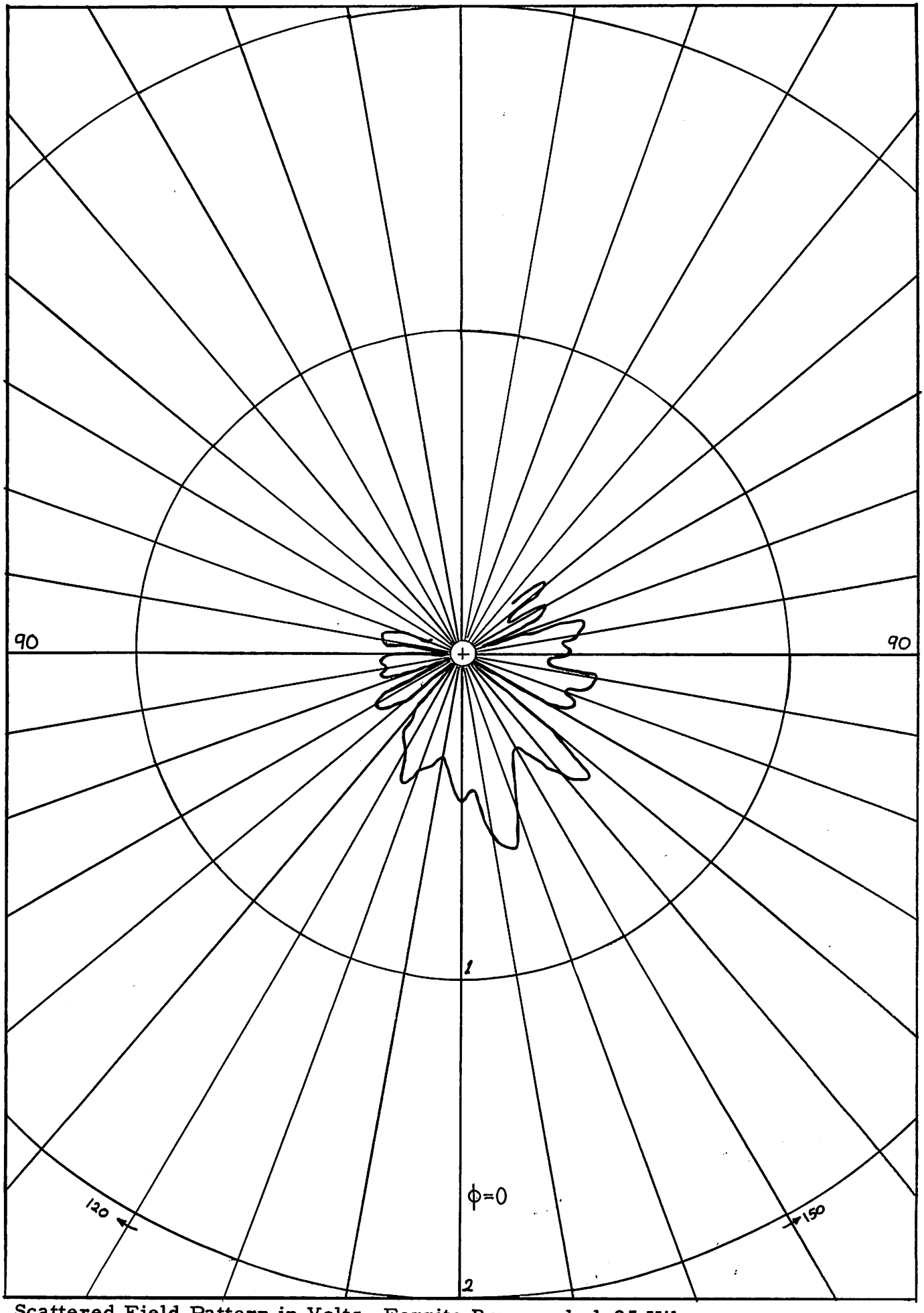

Scattered Field Pattern in Volts, Ferrite Reversed, 1.95 Kilogauss Reversed dc Magnetic Field; Samples: 3"/16 Ferrite Post

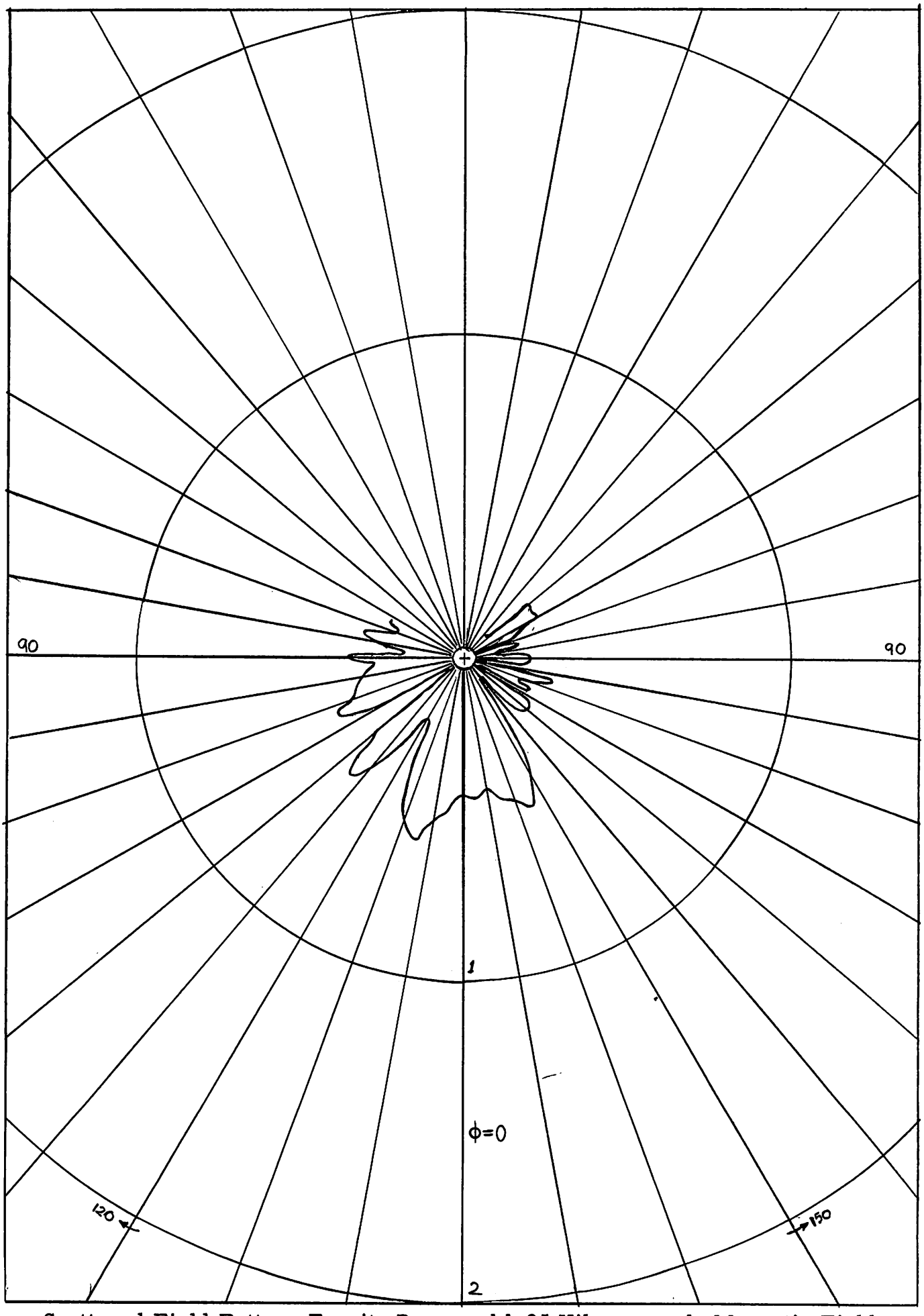

Scattered Field Pattern Ferrite Reversed 1.95 Kilogauss dc Magnetic Field
Sample = 3"/16 Ferrite Post

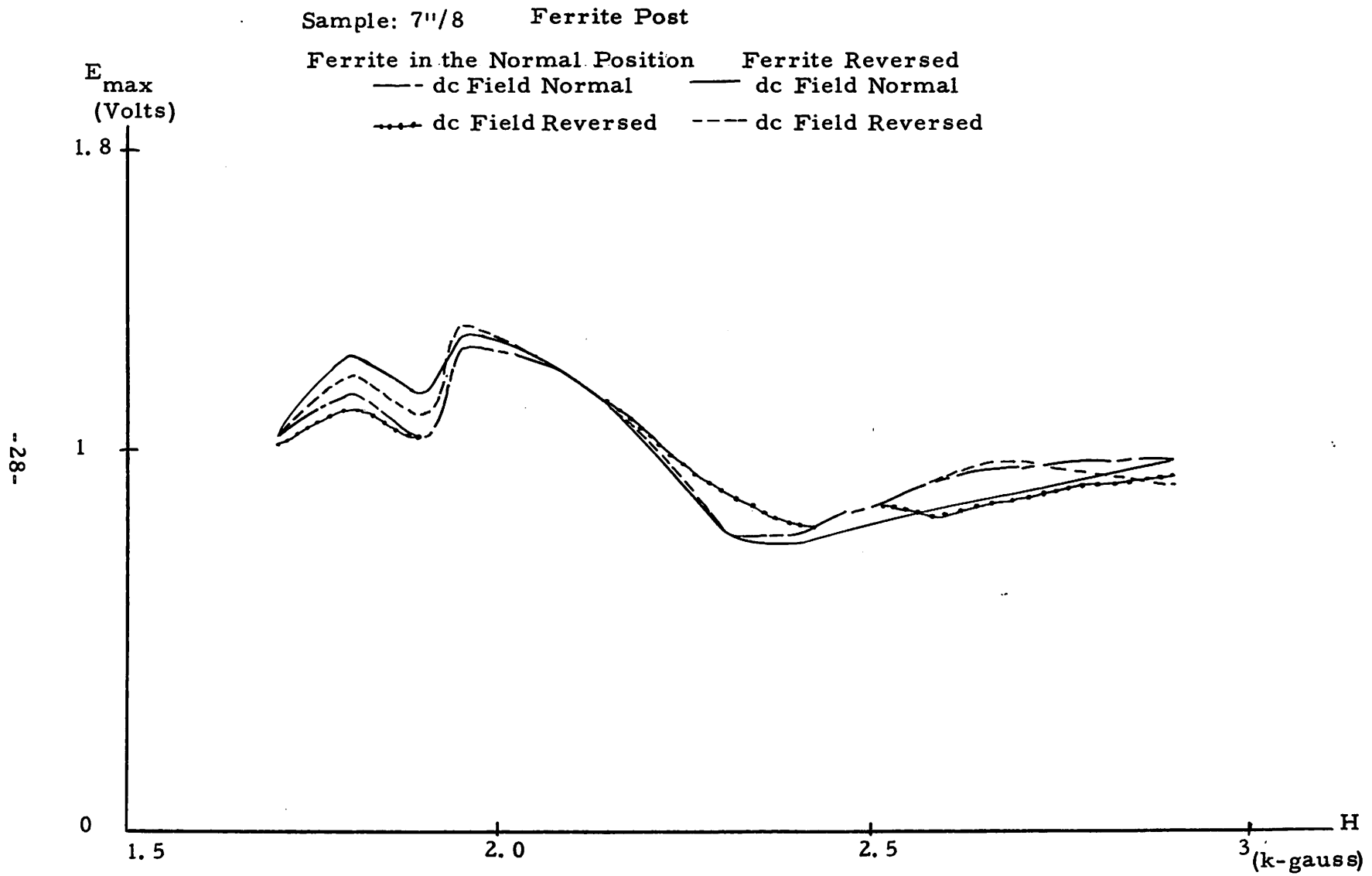
Sample: 7"/8 Ferrite Post
Ferrite in the Normal Position
dc Field Normal
dc Field Reversed
Ferrite Reversed
dc Field Normal
dc Field Reversed
E max (Volts)
1.8
1
0
1.5
2.0
2.5
3
H
(k-gauss)

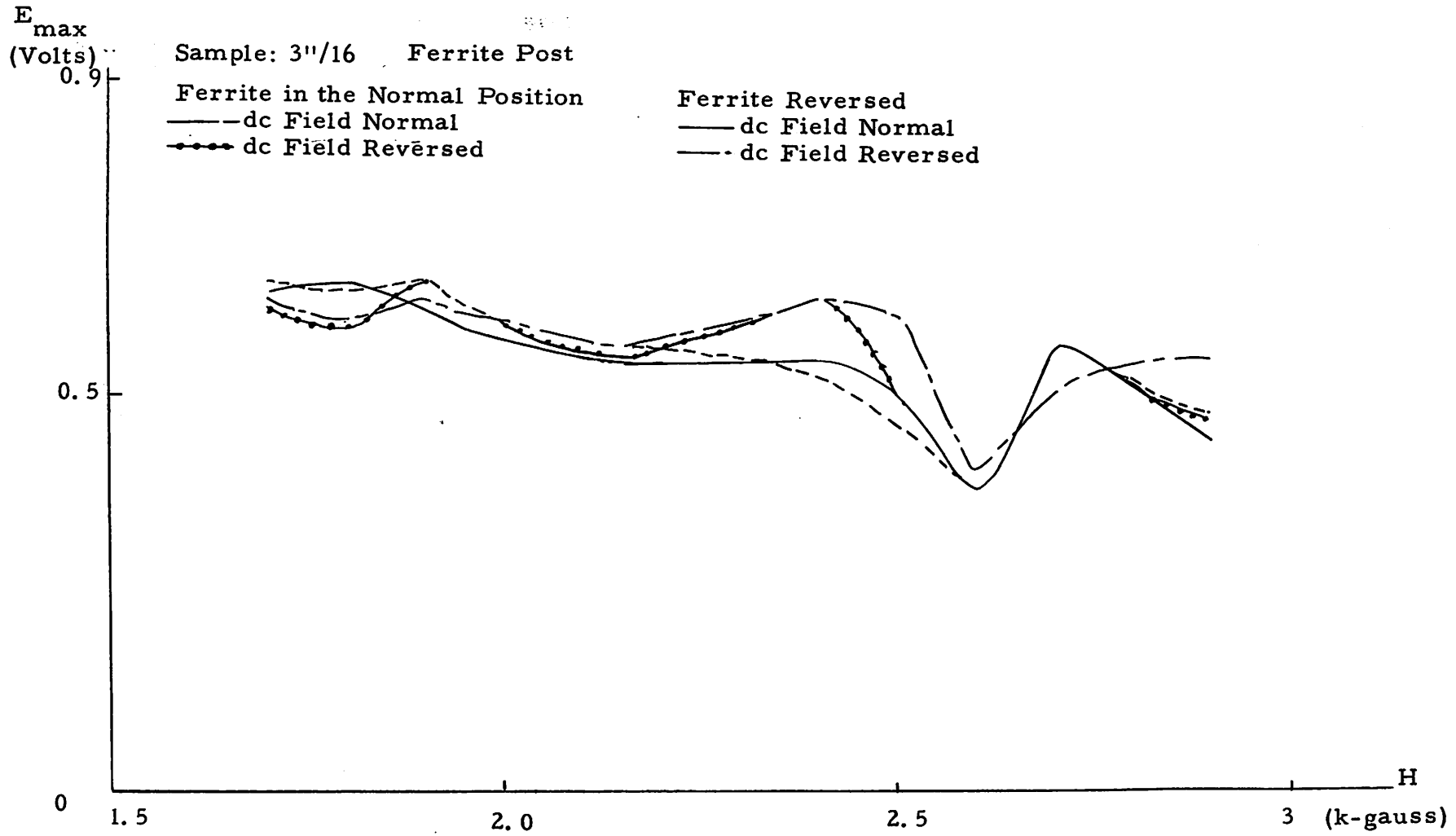
E_{max}
(Volts)
Sample: 3"/16 Ferrite Post
0.9
Ferrite in the Normal Position
dc Field Normal
dc Field Reversed
Ferrite Reversed
dc Field Normal
dc Field Reversed
0.5
0
1.5
2.0
2.5
3
H
(k-gauss)

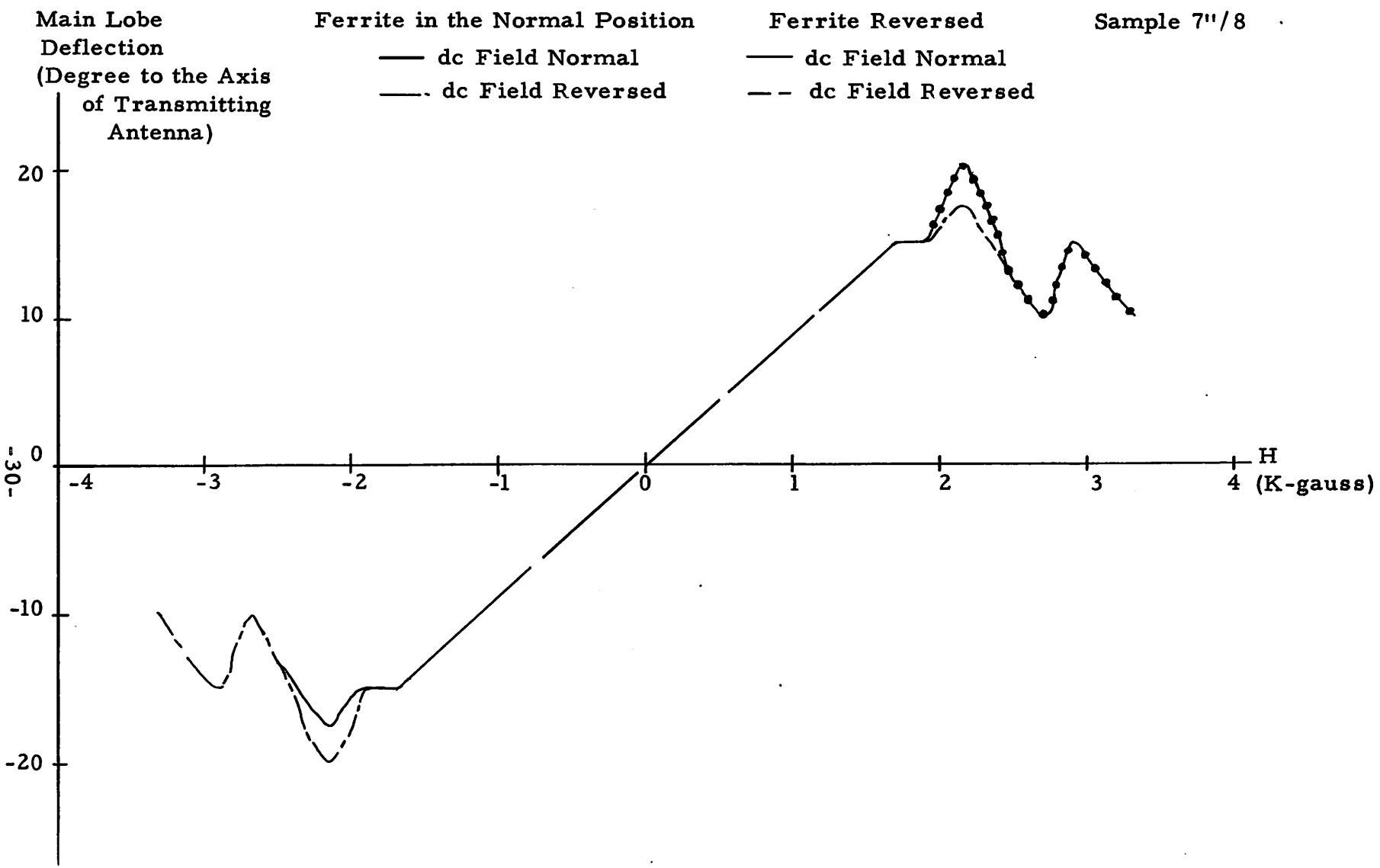
Main Lobe Deflection (Degree to the Axis of Transmitting Antenna)
Ferrite in the Normal Position
dc Field Normal
dc Field Reversed
Ferrite Reversed
dc Field Normal
dc Field Reversed
Sample 7"/8
20
10
0
-10
-20
-30
-4
-3
-2
-1
0
1
2
3
4
H
(K-gauss)

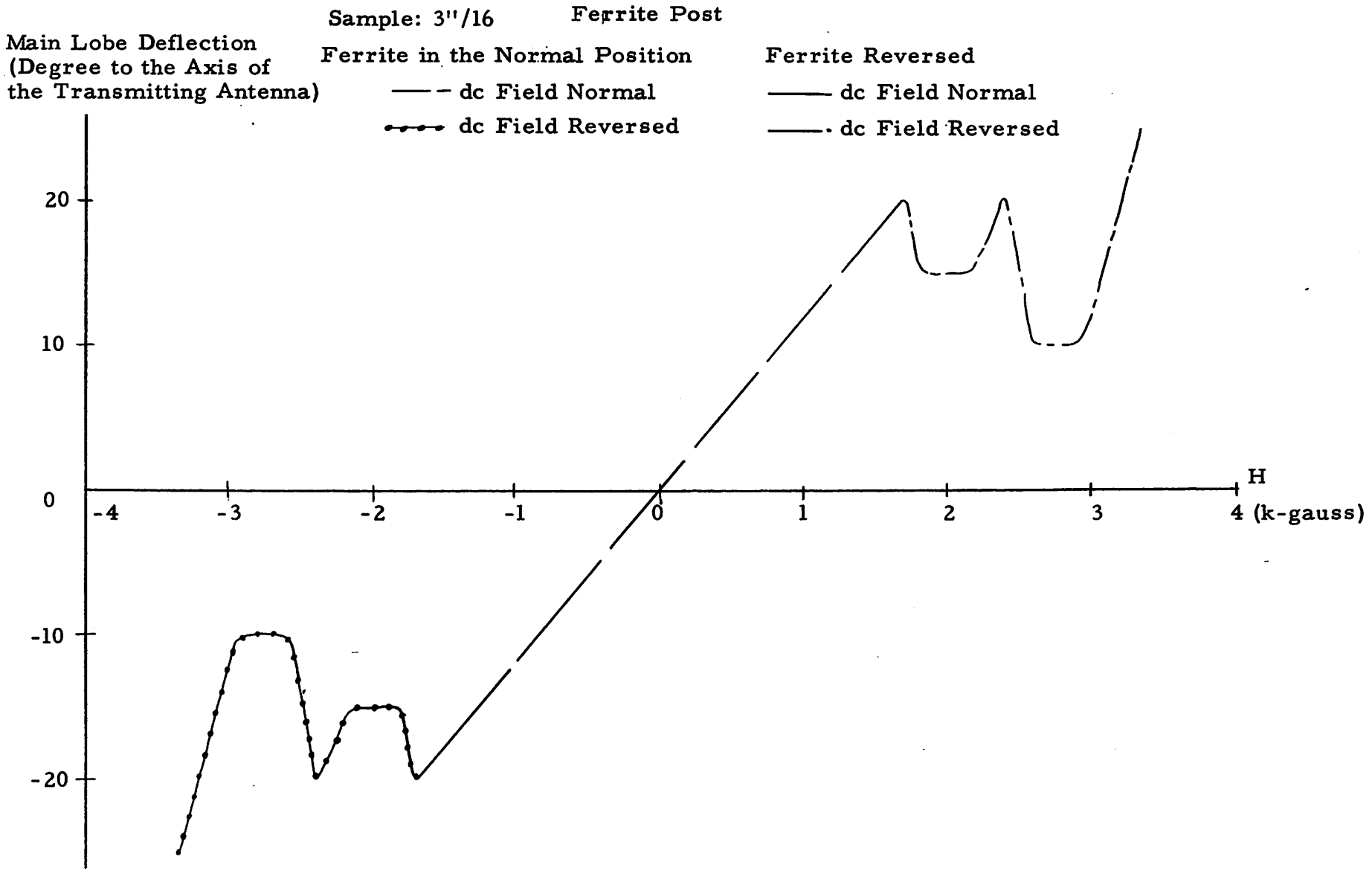
Sample: 3"/16 Ferrite Post
Main Lobe Deflection
(Degree to the Axis of
the Transmitting Antenna)
Ferrite in the Normal Position
dc Field Normal
dc Field Reversed
Ferrite Reversed
dc Field Normal
dc Field Reversed
20
10
0
-10
-20
-4
-3
-2
-1
0
1
2
3
4 (k-gauss)
H

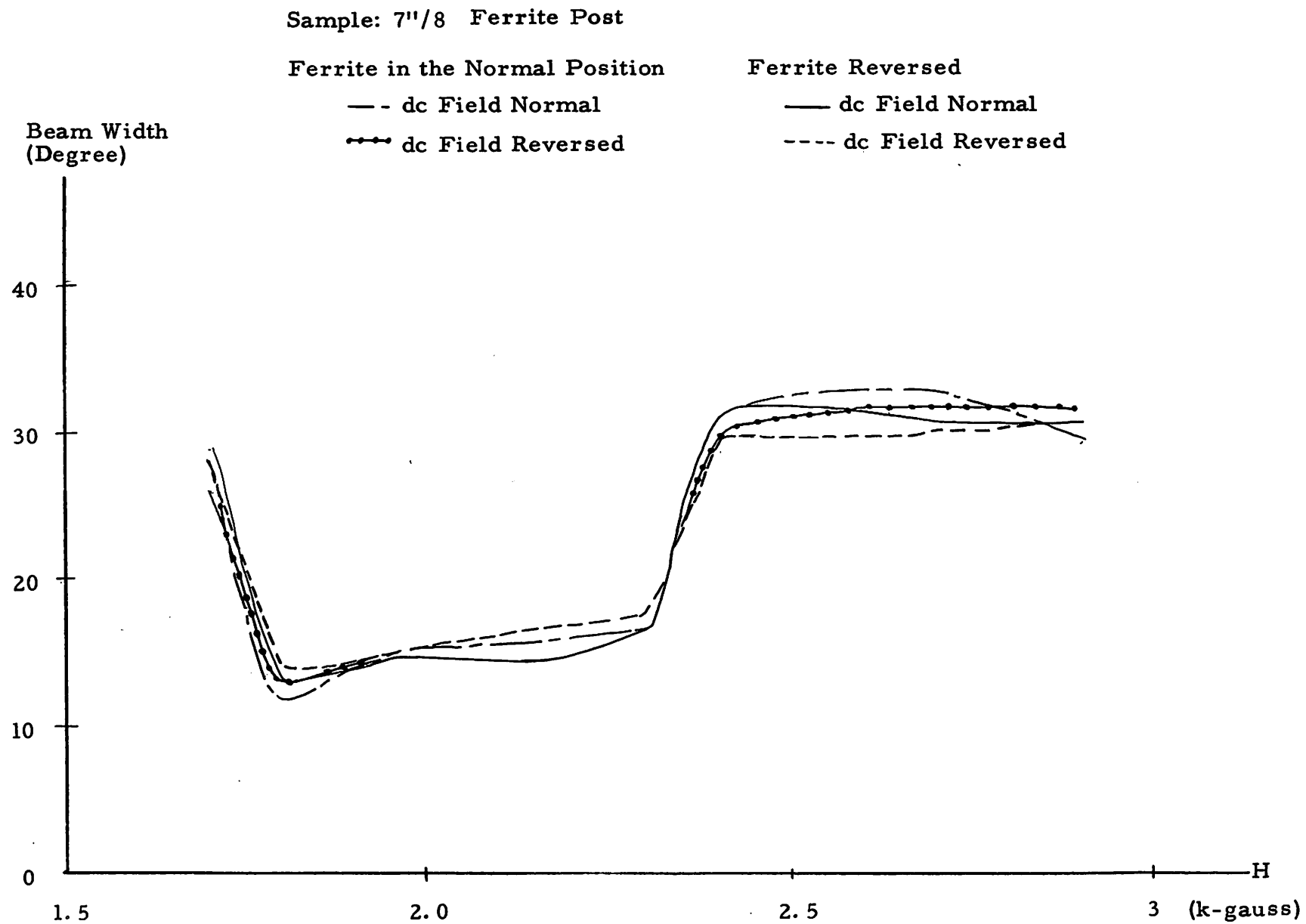
Sample: 7"/8 Ferrite Post
Ferrite in the Normal Position
— - dc Field Normal
•—•—• dc Field Reversed
Ferrite Reversed
—— dc Field Normal
---- dc Field Reversed
Beam Width
(Degree)
40
30
20
10
0
H
1.5
2.0
2.5
3
(k-gauss)

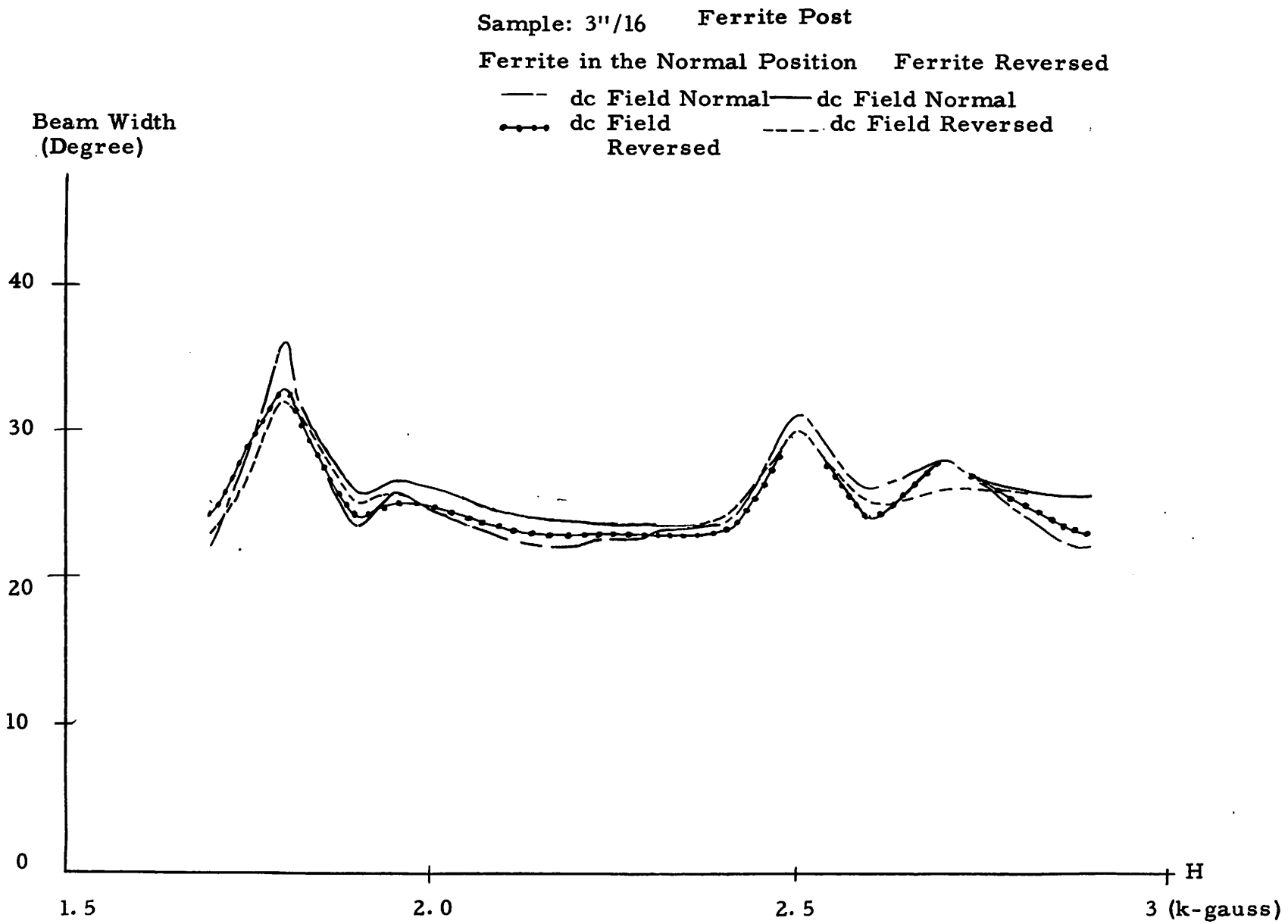
Sample: 3"/16 Ferrite Post
Ferrite in the Normal Position Ferrite Reversed
dc Field Normal
dc Field Normal
dc Field Reversed
dc Field Reversed
Beam Width (Degree)
40
30
20
10
0
H
1.5
2.0
2.5
3 (k-gauss)

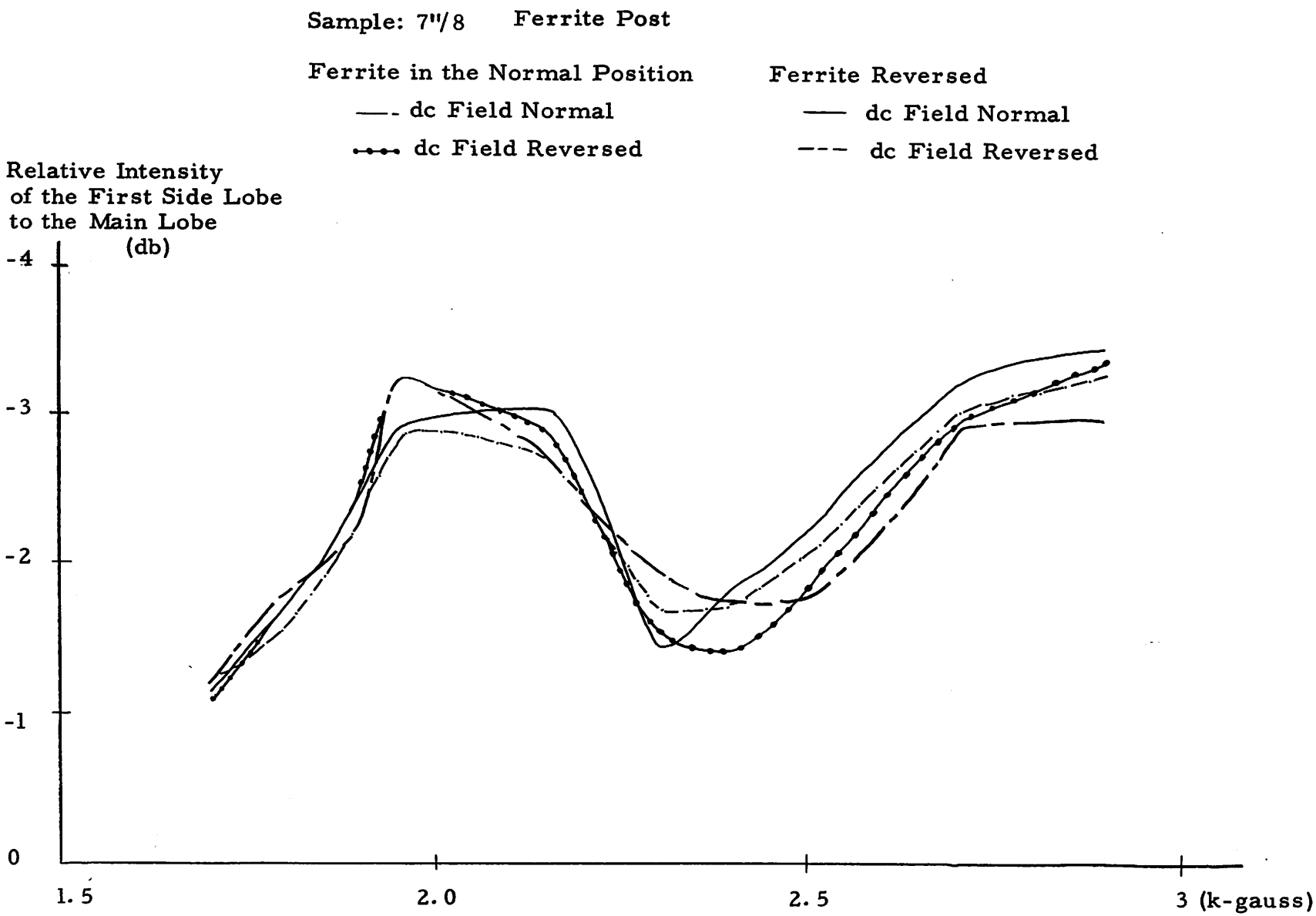
Sample: 7"/8 Ferrite Post
Ferrite in the Normal Position
dc Field Normal
dc Field Reversed
Ferrite Reversed
dc Field Normal
dc Field Reversed
Relative Intensity of the First Side Lobe to the Main Lobe (db)
-4
-3
-2
-1
0
1.5
2.0
2.5
3 (k-gauss)

Sample: 3"/16 Ferrite Post

Ferrite in the Normal Position — Ferrite Reversed

— -dc Field Normal ——— dc Field Normal

•••••• dc Field Reversed – – – – dc Field Reversed

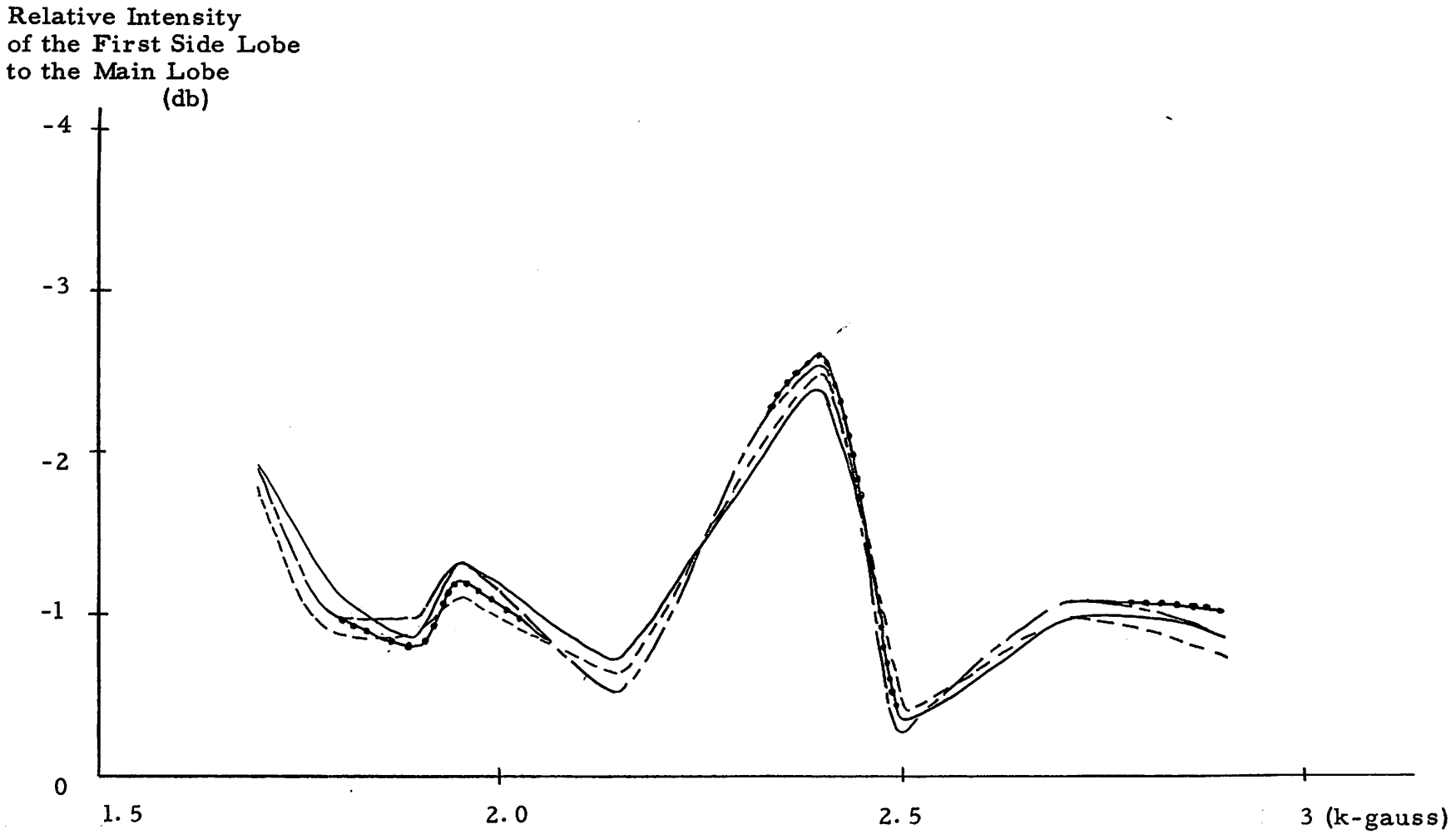

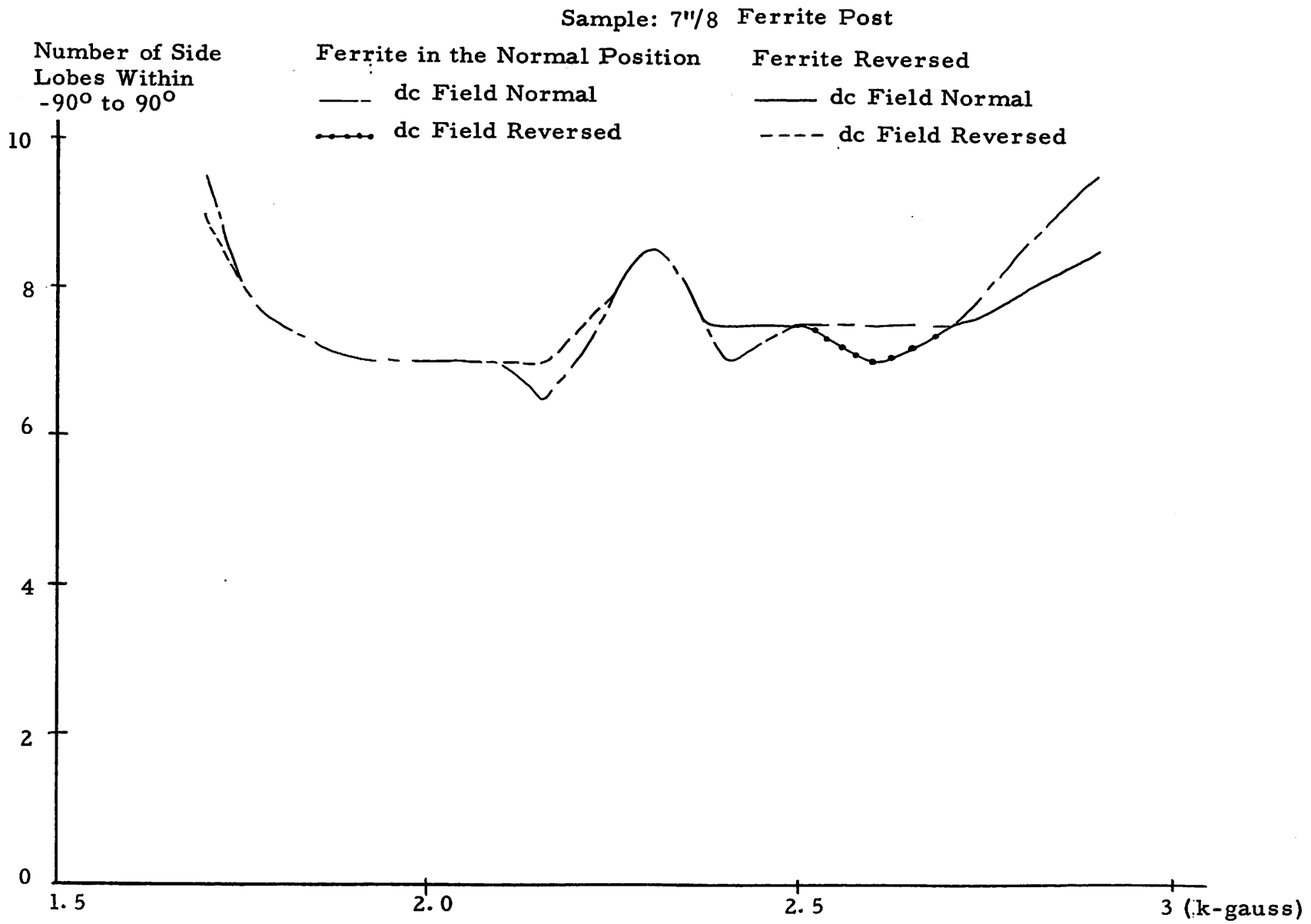
Sample: 7"/8 Ferrite Post
Number of Side Lobes Within -90° to 90°
Ferrite in the Normal Position
dc Field Normal
dc Field Reversed
Ferrite Reversed
dc Field Normal
dc Field Reversed
10
8
6
4
2
0
1.5
2.0
2.5
3 (k-gauss)

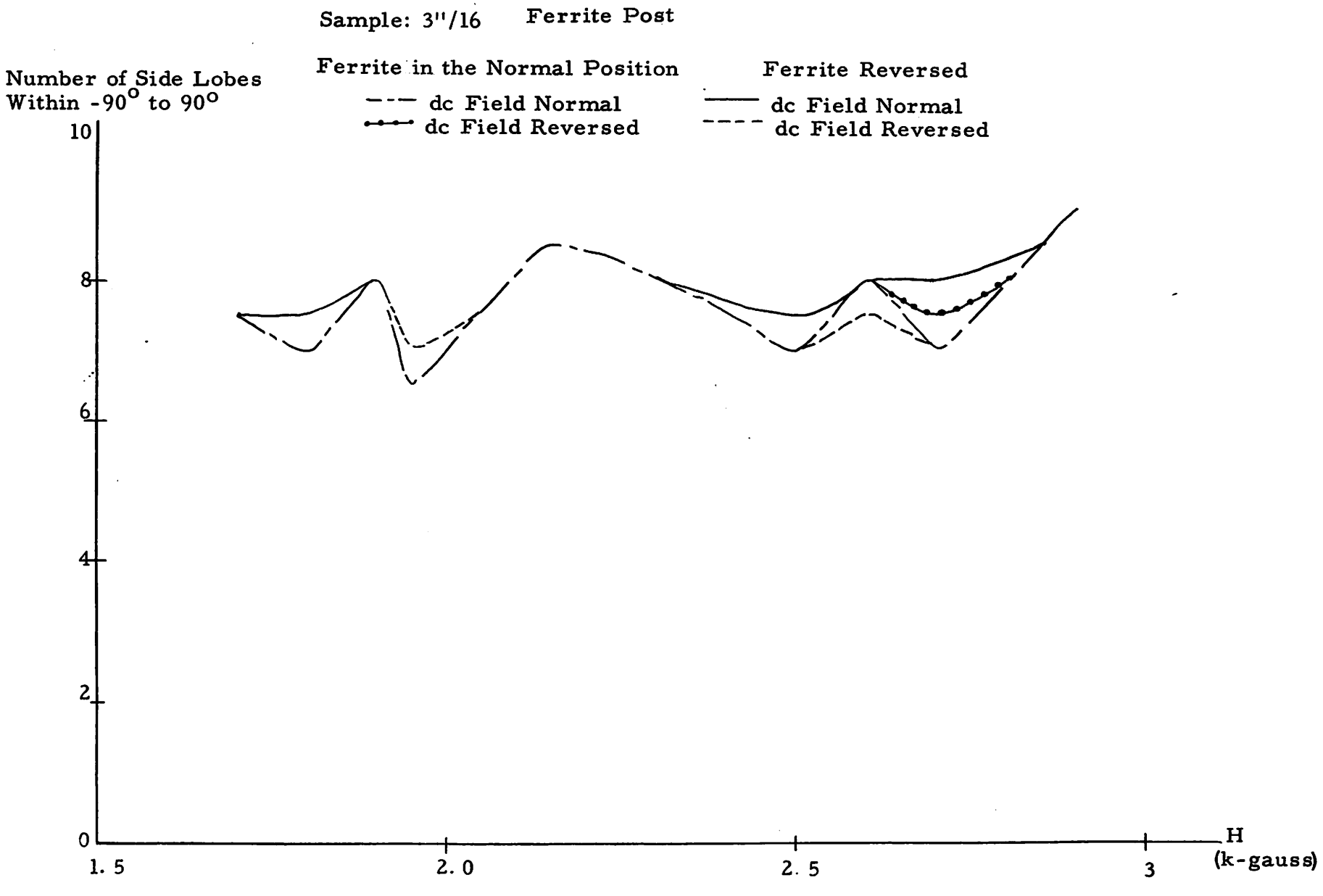
Sample: 3"/16 Ferrite Post
Ferrite in the Normal Position
dc Field Normal
dc Field Reversed
Ferrite Reversed
dc Field Normal
dc Field Reversed
Number of Side Lobes
Within -90° to 90°
10
8
6
4
2
0
1.5
2.0
2.5
3
H
(k-gauss)

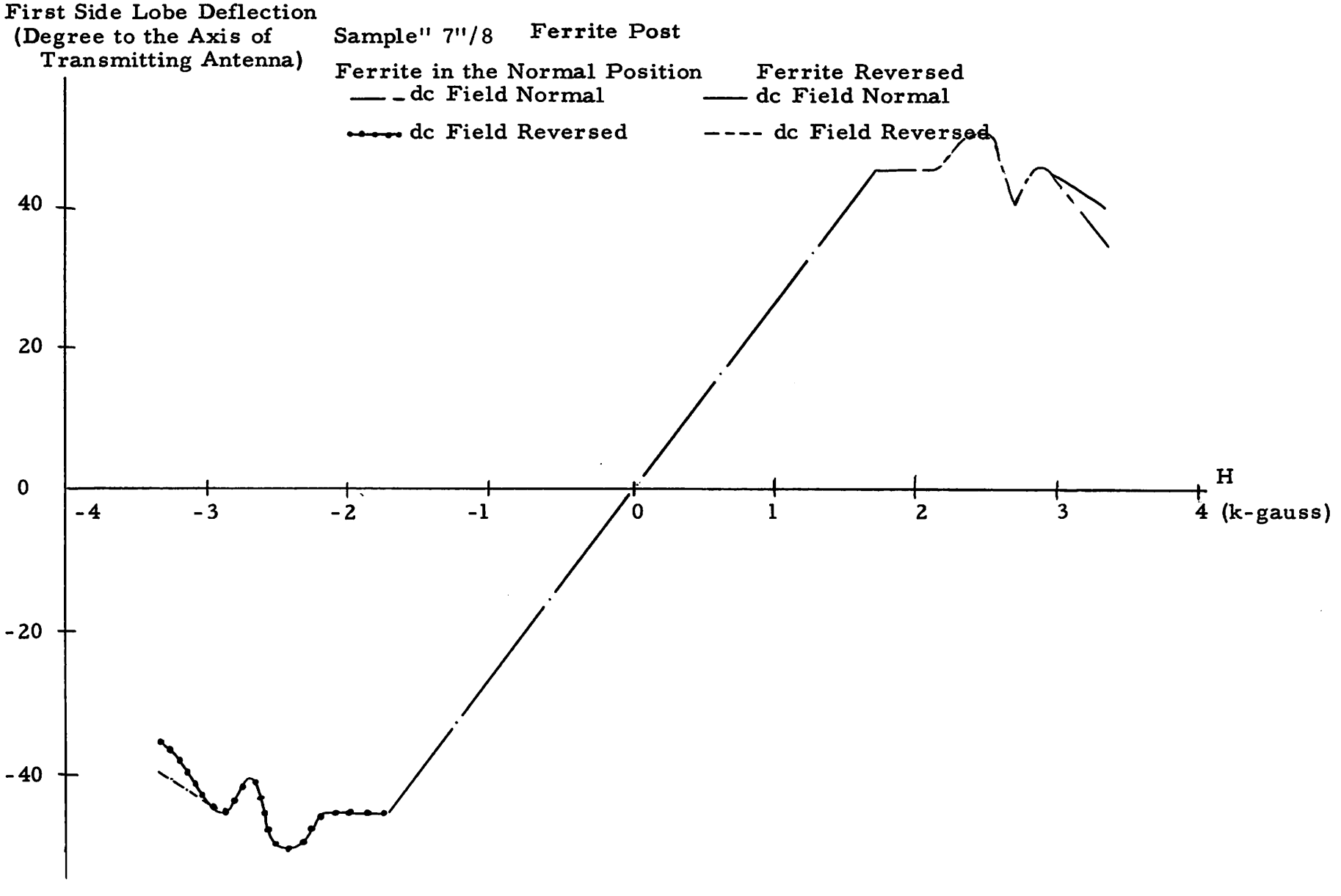
First Side Lobe Deflection
(Degree to the Axis of
Transmitting Antenna)
Sample" 7"/8 Ferrite Post
Ferrite in the Normal Position
dc Field Normal
dc Field Reversed
Ferrite Reversed
dc Field Normal
dc Field Reversed
40
20
0
-20
-40
-4
-3
-2
-1
0
1
2
3
4
H
(k-gauss)

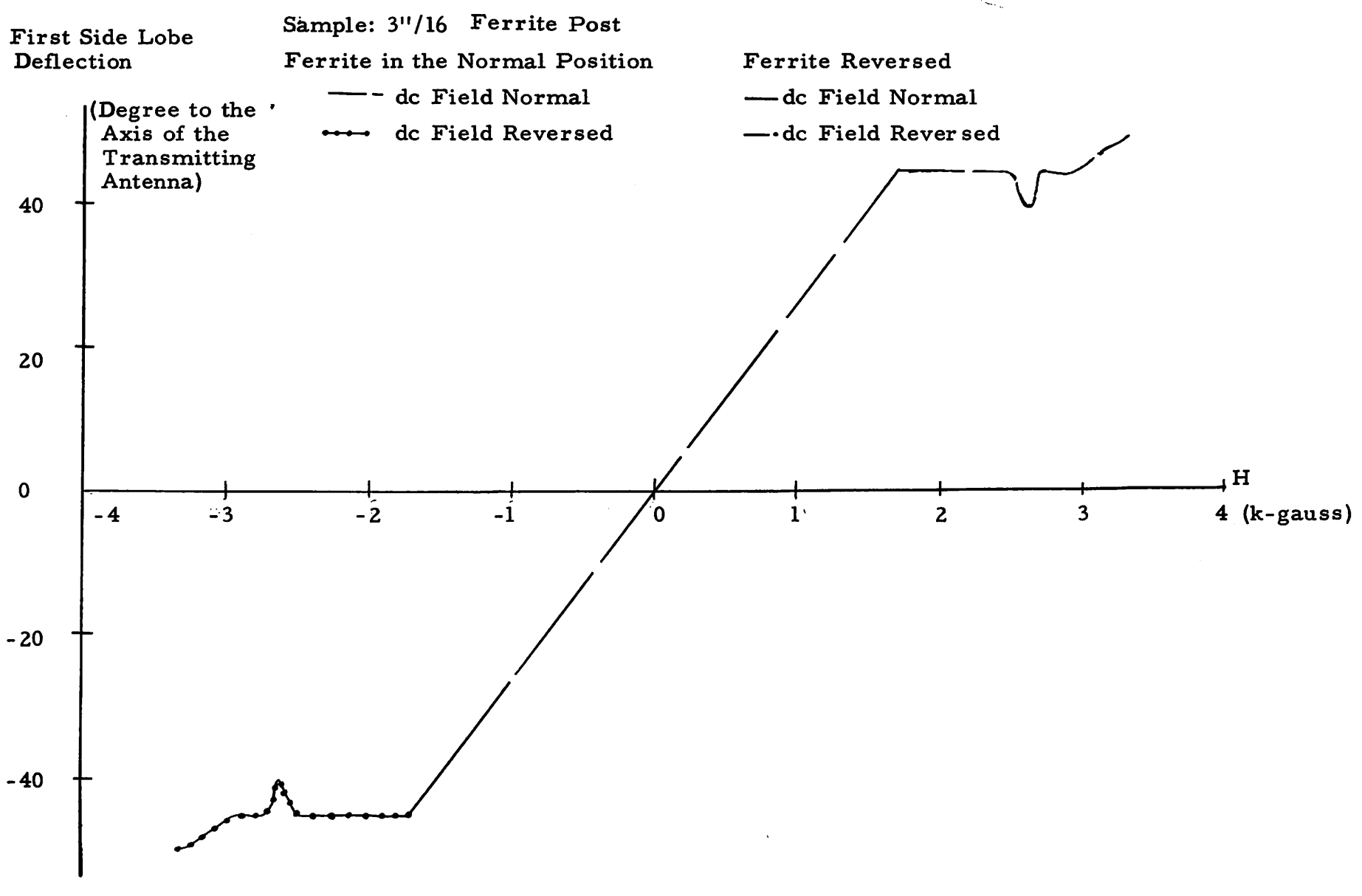
First Side Lobe Deflection
(Degree to the Axis of the Transmitting Antenna)
Sample: 3"/16 Ferrite Post
Ferrite in the Normal Position
dc Field Normal
dc Field Reversed
Ferrite Reversed
dc Field Normal
dc Field Reversed
40
20
0
-20
-40
-4
-3
-2
-1
0
1
2
3
4 (k-gauss)
H

REFERENCES

1. Polder, D., "On the Theory of Ferromagnetic Resonance," Phil. Mag., Vol. 40 (1949), p. 99.
2. Eggimann, W. H., "Scattering of a Plane Wave on a Ferrite Cylinder at Normal Incidence," IRE Trans., M.I.T., Vol. 8, No. 4 (July 1960), p. 440.
3. Clarricoats, P. J. B., Microwave Ferrites, New York: John Wiley, 1961.
4. Soohoo, R. F., Theory and Application of Ferrite, New York: Prentice-Hall Incorp., 1960.
5. Rumsey, V. H., Class Notes, 1961.